Asynchronous CDMA Systems with Random Spreading—Part I: Fundamental Limits

Laura Cottatellucci, Ralph Müller, Merouane Debbah

Asynchronous CDMA Systems with Random Spreading–Part I: Fundamental Limits

Laura Cottatellucci, Ralf R. Müller, and Merouane Debbah

Abstract

Spectral efficiency for asynchronous code division multiple access (CDMA) with random spreading is calculated in the large system limit. We allow for arbitrary chip waveforms and frequency-flat fading. Signal to interference and noise ratios (SINRs) for suboptimal receivers, such as the linear minimum mean square error (MMSE) detectors, are derived. The approach is general and optionally allows even for statistics obtained by under-sampling the received signal.

All performance measures are given as a function of the chip waveform and the delay distribution of the users in the large system limit. It turns out that synchronizing users on a chip level impairs performance for all chip waveforms with bandwidth greater than the Nyquist bandwidth, e.g. positive roll-off factors. For example, with the pulse shaping demanded in the UMTS standard, user synchronization reduces spectral efficiency up to 12% at 10 dB normalized signal-to-noise ratio. The benefits of asynchronism stem from the finding that the excess bandwidth of chip waveforms actually spans additional dimensions in signal space, if the users are de-synchronized on the chip-level.

The analysis of linear MMSE detectors shows that the limiting interference effects can be decoupled both in the user domain and in the frequency domain such that the concept of the effective interference spectral density arises. This generalizes and refines Tse and Hanly's concept of effective interference.

In Part II, the analysis is extended to any linear detector that admits a representation as multistage detector and guidelines for the design of low complexity multistage detectors with universal weights are provided.

Index Terms - Asynchronous code division multiple access (CDMA), channel capacity, multiuser detection, random matrix theory, effective interference, linear minimum mean square error (MMSE) detector, multistage detector, random spreading sequences, spectral efficiency, excess bandwidth, pulse shaping.

This work was presented in part at the IEEE Information Theory Workshop (ITW 2006), Punta de l'Este, Uruguay, March 2006 and at the IEEE Wireless Communications and Networking Conference, Hong Kong, March 2007. It partly appears in Laura Cottatellucci, "Low Complexity Multistage Detectors for Randomly Spread CDMA Systems", Ph.D. thesis, Vienna University of Technology, March 2006.

This was supported by the French and Australian Science and Technology (FAST) Programme and the Norwegian Research Council under grant 171133/V30.

Laura Cottatellucci is with Institute Eurecom, Sophia Antipolis, France (e-mail: laura.cottatellucci@eurecom.fr). She was with Institute of Telecommunications Research, University of South Australia, Adelaide, SA, Australia. Ralf Müller was with Forschungszentrum Telekommunikation Wien (ftw.) He is now with Norwegian University of Science and Technology (NTNU), Trondheim, Norway, (e-mail: ralf@iet.ntnu.no). Merouane Debbah was with Institut Eurecom, Sophia Antipolis, France. Currently, he is with SUPELEC, Paris, France (e-mail: merouane.debbah@supelec.fr).

I. INTRODUCTION

The fundamental limits of synchronous code-division multiple-access (CDMA) systems and the loss incurred by the imposition of suboptimal receiving structures have been thoroughly studied in different scenarios and from different perspectives. On the one hand, significant efforts have been devoted to characterize the optimal spreading sequences and the corresponding capacities [1], [2], [3]. On the other hand, very insightful analysis [4], [5], [6], [7], [8] resulted from modelling the spreading sequences by random sequences [9]. In fact, as both the K transmitted signals and the spreading factor N tend to infinity with a fixed ratio, CDMA systems with random spreading show self-averaging properties. These enable the description of the system in terms of few macroscopic system parameters and thus provide a deep understanding of the system behavior.

In the literature, the fundamental limits of CDMA systems and the asymptotic analysis of linear multiuser detectors under the assumption of random spreading sequences is overwhelmingly focused on synchronous CDMA systems. While the assumption of user synchronization allowed for accurate large-system analysis, it is not realistic for the received signal on the uplink of a cellular CDMA system, in particular if users move and cause varying delays. Therefore, it is of theoretical and practical interest to extend the analysis of CDMA systems with random spreading to asynchronous users. This holds in particular, as we will see that from a viewpoint of system performance, asynchronous users are beneficial.

The analysis of asynchronous CDMA systems using a single-user matched filter as receiver was first given in [10]. A rich field of analysis of asynchronous CDMA systems with conventional detection at the receiver is based on Gaussian approximation methods. An exhaustive overview of these approaches exceeds the scope of this work, which is focused on the analysis of asynchronous CDMA systems with *optimal joint decoding or linear multiuser detection*. The interested reader is referred to [11] [12] and references therein for asynchronous CDMA with single-user receivers.

The analysis and design of asynchronous CDMA systems with linear detectors is predominantly restricted to consider symbol-asynchronous but chip-synchronous signals, i.e. the time delays of the signals are multiples of the chip interval. The effect of chip-asynchronism is eventually analyzed independently [13]. In this stream are works that optimize the spreading sequences to maximize the sum capacity [14] and analyze the performance of linear multiuser detectors [13], [15], [16], [17]. In [13], [15], the linear MMSE detector for symbol-asynchronous but chip-synchronous systems is shown to attain the performance of the linear MMSE detector for synchronous systems as the size of the observation window tends to infinity by empirical

and analytical means, respectively. However, they verify numerically that the performance of linear MMSE detectors is severely impaired by the use of short observation windows. Additionally, [15] provides the large-system SINR for a symbol whose chips are completely received in an observation window of length equal to the symbol interval T_s. In [16], [17], the analysis of linear multistage and MMSE detectors is extended to observation windows of arbitrary length. Furthermore, a multistage detector structure that does not suffer from windowing effects and performs as well as the multistage detector for synchronous systems is proposed.

In [13], [18], the effects of chip asynchronism are analyzed assuming bandlimited chip pulses. In [18], the chip waveform is assumed to be an ideal Nyquist sinc function, i.e. a sinc function with bandwidth equal to half of the chip rate. The received signal is filtered by a lowpass filter (or, equivalently, a filter matched to the chip waveform) and subsequently sampled at the time delay of the signal of the user of interest with a frequency equal to the chip rate[1]. Reference [18] proves that the SINR at the output of the linear MMSE detector converges in the mean-square sense to the SINR in an equivalent synchronous system. In [13] the wider class of chip pulses which are inter-chip interference free at the output of the chip matched filter is considered. In the following we will refer to this class of chip pulses as square root Nyquist chip pulses.

In [19], [20], the performance of the linear MMSE detector with completely asynchronous users and chip waveforms limited to a chip interval is analyzed. However, the observation window in [19] spanned only a single symbol interval not yielding sufficient discrete-time statistics; the resulting degradation in performance was pointed out later in [13], [15].

As discussed above, previous approaches to the analysis of asynchronous CDMA with multiuser detection were only concerned with, if and how asynchronism can be prevented from causing performance degradation. However, asynchronism is known to be beneficial for CDMA systems with demodulation by single-user matched filters (e.g. [10]). It is the main contribution of this paper to show that benefits from asynchronism are not inherent to single-user matched filters but a general property of CDMA systems and to quantify those benefits in the large-system limit.

Compared to synchronous systems, the analysis of asynchronous CDMA raises two additional issues: (i) the way statistics are formed, trading complexity against performance, and (ii) the effects of excess bandwidth, chip-pulse shaping and the users' delay distribution.

The optimum multiuser detector in [21] is based on the sufficient statistics obtained as output samples of

[1]The chip rate satisfies the condition of the sampling theorem in this case.

a bank of filters matched to the symbol spreading waveforms of all users. The decorrelating detector in [22] and the linear MMSE detector in [23] benefit from the same sufficient statistics. A method to determine the eigenvalue moments of a correlation matrix in asynchronous CDMA systems using such statistics and square root Nyquist chip pulse waveforms is proposed in [24].

An alternative approach to generate useful statistics, which in general are not sufficient is borrowed from synchronous systems. The received signals are processed by a filter matched to the chip waveform and sampled at the chip rate. This approach is optimum for single-user communications and chip-synchronous multi-user communications, but causes aliasing to the signals of de-synchronized users if the chip waveform has non-zero excess bandwidth. Discretization schemes using chip matched filters and sampling at the Nyquist rate are studied in [25]. There, the notion of approximate sufficient statistics was introduced. Furthermore, conventional CDMA systems with chip waveforms that approximate sinc pulses were shown to outperform systems using rectangular pulse shaping. Moreover, it was conjectured that sinc pulses are optimal for CDMA systems with linear MMSE multiuser detection.

In systems with bandlimited waveforms, sampling at a rate faster than the Nyquist rate leads to the same performance as the optimal time-discretization proposed in [21], [22], [23] if the condition of the sampling theorem is satisfied [13]. In contrast to the bank of symbol matched filters in [21], this approach has the advantage that the time delays of the users' signals need not be known before sampling.

The impact of the shape and excess bandwidth of the chip pulses received attention in [26], [27], [25]. In [26], [27] an algorithm for the design of chip-pulse waveforms for CDMA systems with *conventional detection* has been proposed. The design criterion consists of minimizing the bit error rate at the output of a *single user matched filter* in asynchronous CDMA systems while enforcing certain constraints on the chip waveforms.

This work is organized in six additional sections. Section II, gives a brief overview of the main results found in this work. Sections III and IV introduce notation and the system model for asynchronous CDMA, respectively. Section V focuses on the analysis of linear MMSE detectors and introduces the main mathematical tools for analysis of the fundamental limits of asynchronous CDMA. In Section VI, the spectral efficiency of optimal joint decoding is derived on the basis of the results for the linear MMSE detector exploiting the duality between mutual information and MMSE. Section VII addresses the extension of the presented results to more general settings. Some conclusions are drawn in Section VIII.

II. MAIN RESULTS

Before going into the main results of this work, it is helpful to get some intuition on asynchronous CDMA systems. First of all, one might be interested in the question which chip waveform gives the highest spectral efficiency for otherwise arbitrary system parameters, like pulse shape, pulse width in time and frequency, system load, etc. There is a surprisingly easy answer to this question that does not require any sophisticated mathematical tools:

Proposition 1 *Nyquist sinc-pulses maximize spectral efficiency for otherwise free system parameters.*

Proof: The proof is by contradiction. First, it is well-known that the spectral efficiency of a single user channel is maximized by Nyquist sinc-pulses. Further, we know from [4] that the spectral efficiency of a synchronous CDMA system with Nyquist sinc-pulses becomes identical to the spectral efficiency of a single user channel, as the load converges to infinity. Finally, the multiuser system can never outperform the single user system, since we could otherwise improve a single user system by virtually splitting the single user into many virtual users. Thus, the Nyquist sinc pulse is optimum also for the multi-user system. ■

Note that, from the previous proof, the Nyquist sinc pulse is optimum for an infinite system load. However, we cannot judge whether the optimum is unique from the line of thought proposed in our proof. In fact, a straightforward application of a more general result in this paper (shown in the Appendix V) is the following:

Proposition 2 *Asynchronous CDMA systems with any sinc-pulses, no matter whether they are constrained to the Nyquist bandwidth or to a larger, or even to a smaller bandwidth, and users whose empirical delays are uniformly distributed within a symbol interval achieve the same spectral efficiency as a single user channel, if the load converges to infinity.*

The optimization of the system load neither gives the theoretically most interesting cases to consider nor the practically most relevant. Let us, thus, look at which chip waveforms achieve the highest spectral efficiency for a fixed load. Surprisingly, the result is not a little bit more useful for practical applications:

Corollary 1 *The chip waveform that maximizes the spectral efficiency for a given finite load and given chip*

rate has vanishing bandwidth. Furthermore, the maximum spectral efficiency is the same as the one for the single user channel.

Proof: The corollary follows directly from Proposition 2. Note that Proposition 2 holds for an arbitrary chip rate and an arbitrary bandwidth of the chip waveform and states that the single user bound is reached at infinite load. Though, the corollary is stated for a given finite load, we are free to split each physical user into M virtual users and let M increase to infinity such that the virtual load becomes infinite. Therefore, we take a user's signal and divide it into M data streams that are time-multiplexed in such a way as to result in the same physical transmit signal for that user. Applying this idea to each of the K physical users, we have created MK virtual users. Furthermore, the chip interval has grown from T_c to MT_c and the virtual users are asynchronous with a discrete uniform distribution of delays within the virtual chip interval of length MT_c. Consider now a sinc pulse of bandwidth $1/(2MT_c)$ as chip waveform. If we take the limit $M \to \infty$ for the system of virtual users, the delay distribution converges to the uniform distribution within the virtual chip interval and the number of virtual users converges to infinity. Thus, Proposition 2 applies and the single user bound is reached. Therefore, this choice of chip waveforms whose bandwidth vanishes is optimal. ■

Optimizing chip waveforms to maximize spectral efficiency has proven to hardly aid the practical design of CDMA systems, since the optima are achieved for system parameters, e.g. infinite load and/or vanishing bandwidth, that are far from the limits of practical implementation. Furthermore, the choice of the chip waveform is influenced by many other factors than spectral efficiency like the difficulty to implement steeply decaying frequency filters and the need to keep the peak-to-average power ratio of the continuous-time transmit signal moderate. Therefore, many commercial CDMA systems, e.g. the Universal Mobile Telecommunication System (UMTS), use chip waveforms with excess bandwidth. The UMTS standard uses root-raised cosine pulses with roll-off factor 0.22. Motivated by the theoretical findings above and the practical constraints on the design of chip waveforms, the rest of this paper puts the focus on the performance analysis of CDMA system with a given fixed chip waveform. As it will be seen, this gives rise to a rich collection of insights into CDMA systems with asynchronous users. The main results are summarized in the following.

CDMA systems using chip pulse waveforms with bandwidth B not greater than half of the chip rate $\frac{1}{T_c}$, i.e. $B \leq \frac{1}{2T_c}$, perform identically irrespective of whether the users are synchronized or not for a large class of performance measures. Furthermore, our result generalizes the equivalence result for the ideal Nyquist sinc waveform (with bandwidth $\frac{1}{2T_c}$) in [18] to any chip pulse satisfying the mentioned bandwidth constraint and

to any linear multistage detector and the optimal capacity-achieving joint decoder. Note that the performance is independent of the time delay distribution. Increasing the bandwidth of the chip waveform above $\frac{1}{2T_c}$, i.e. allowing for some excess bandwidth as it is customary in all implemented systems, the behaviors of CDMA systems change substantially. They depend on the time delay distribution and the equivalence between synchronous and asynchronous systems is lost.

For any choice of chip waveform, we capture the performance of a large CDMA system with linear MMSE detection by a positive definite frequency-dependent Hermitian matrix $\Upsilon(\Omega)$ whose size is the ratio of sampling rate to chip rate (the sampling rate is a multiple of the chip rate). We require neither the absence of inter-chip interference, nor that the samples provide sufficient statistics, nor a certain delay distribution. Unlike for synchronous users, the multiuser efficiency [28] in the large-system limit is not necessarily unique for all users. The matrix $\Upsilon(\Omega)$ reduces to a scalar frequency dependent function $\eta(\omega)$ in cases where oversampling is not needed. Interestingly, the same holds true even in cases with excess bandwidth if the delay distribution is uniform. The scalar $\eta(\omega)$ can be understood as a multiuser efficiency spectral density with the multiuser efficiency being its integral over frequency ω. We find that in large systems, the effects of interference from different users and interference at different frequencies decouple. We, thus, generalize Tse and Hanly's [5] concept of effective interference to the concept of effective interference spectral density which decouples the effects of interference in both user and frequency domain.

Excess bandwidth can be utilized if users are asynchronous. While excess bandwidth is useless for synchronized systems in terms of multiuser efficiency, i.e. all square root Nyquist pulses perform the same regardless of their bandwidth, desynchronizing users improves the performance of any system with non-vanishing excess bandwidth.

III. NOTATION AND SOME USEFUL DEFINITIONS

Throughout this work, upper and lower boldface symbols are respectively used for matrices and vectors spanning a single symbol interval. Matrices and vectors describing signals spanning more than a symbol interval are denoted by upper boldface calligraphic letters.

In the following, we utilize *unitary* Fourier transforms both in the continuous time and in the discrete time domain. The unitary Fourier transform of a signal $s(t)$ in the continuous time domain is given by $S(\omega) = \frac{1}{\sqrt{2\pi}} \int_{-\infty}^{+\infty} s(t) \mathrm{e}^{-j\omega t} \mathrm{d}t$. The unitary Fourier transform of a sequence $\{\ldots, c_{-1}, c_0, c_1, \ldots\}$ in the discrete time domain is given by $c(\Omega) = \frac{1}{\sqrt{2\pi}} \sum_{n=-\infty}^{+\infty} c_n \mathrm{e}^{-j\Omega n}$. We will refer to them shortly as Fourier

transform. Throughout this work, ω and Ω denote the angular frequency and the normalized angular frequency, respectively. A function in Ω has support in the interval $[-\pi, \pi]$, or translations of it.

For further studies it is convenient to define the concept of *r-block-wise circulant matrices of order N*:

Definition 1 *Let r and N be positive integers. An r-block-wise circulant matrix of order N is an $rN \times N$ matrix of the form*

$$\boldsymbol{C} = \begin{pmatrix} \boldsymbol{B}_0 & \boldsymbol{B}_1 & \cdots & \boldsymbol{B}_{N-1} \\ \boldsymbol{B}_{N-1} & \boldsymbol{B}_0 & \cdots & \boldsymbol{B}_{N-2} \\ \vdots & \vdots & & \vdots \\ \boldsymbol{B}_1 & \boldsymbol{B}_2 & \cdots & \boldsymbol{B}_0 \end{pmatrix} \tag{1}$$

with $\boldsymbol{B}_i = (c_{1,i}, c_{2,i}, \ldots, c_{r,i})^T$.

In the matrix $\boldsymbol{C}$, an $r \times N$ block row is obtained by a circular right shift of the previous block. Since the matrix $\boldsymbol{C}$ is univocally defined by the unitary Fourier transforms of the sequences

$$c_s(\Omega) = \frac{1}{\sqrt{2\pi}} \sum_{k=0}^{N-1} c_{s,k} \mathrm{e}^{-j\Omega k} \qquad s = 1, \ldots, r, \tag{2}$$

there exists a bijection $\mathfrak{F}$ from the frequency dependent vector $\boldsymbol{c}(\Omega) = [c_1(\Omega), c_2(\Omega), \ldots, c_r(\Omega)]$ to $\boldsymbol{C}$. Thus,

$$\mathfrak{F}\{\boldsymbol{c}(\Omega)\} = \boldsymbol{C}. \tag{3}$$

Furthermore, the superscripts $\cdot^T$ and $\cdot^H$ denote the transpose and the conjugate transpose of the matrix argument, respectively. $\boldsymbol{I}_n$ is the identity matrix of size $n \times n$ and $\mathbb{C}$, $\mathbb{Z}$, $\mathbb{Z}^+$, $\mathbb{N}$, and $\mathbb{R}$ are the fields of complex, integer, nonnegative integer, positive integer, and real numbers, respectively. $\mathrm{tr}(\cdot)$, $\|\cdot\|$, and $|\cdot|$ are the trace, the Frobenius norm, and the spectral norm of the argument, respectively, i.e. $\|\mathbf{A}\| = \sqrt{\mathrm{tr}(\mathbf{A}\mathbf{A}^H)}$, $|\mathbf{A}| = \max_{\mathbf{x}^H\mathbf{x} \leq 1} \mathbf{x}^H \mathbf{A}\mathbf{A}^H \mathbf{x}$. $\mathrm{diag}(\cdot) : \mathbb{C}^n \mapsto \mathbb{C}^{n \times n}$ transforms an n-dimensional vector into a diagonal matrix of size $n \times n$ having as diagonal elements the components of the vector in the same order. $\mathrm{E}\{\cdot\}$ and $\Pr\{\cdot\}$ are the expectation and probability operators, respectively. δ_{ij} is the Kronecker symbol and $\delta(\lambda)$ is Dirac's delta function. $\boldsymbol{X} = (x_{ij})_{i=1,\ldots,n_1}^{j=1,\ldots,n_2}$ is the $n_1 \times n_2$ matrix whose (i,j)-element is the scalar x_{ij}. $\boldsymbol{X} = (\boldsymbol{X}_{ij})_{i=1,\ldots,n_1}^{j=1,\ldots,n_2}$ is the $n_1 q_1 \times n_2 q_2$ block matrix whose (i,j)-block is the $q_1 \times q_2$ matrix $\boldsymbol{X}_{ij}$. The notation $\lfloor \cdot \rfloor$ is adopted for the operator that yields the maximum integer not greater than its argument and $x \mathrm{mod} y$ denotes the modulus, i.e. $x \mathrm{mod} y = x - \left\lfloor \frac{x}{y} \right\rfloor x$. Furthermore, $\chi(\boldsymbol{x} \in \mathcal{A})$ denotes the indicator function of the variable $\boldsymbol{x}$ on the set $\mathcal{A}$ and $\chi(\boldsymbol{x} \in \mathcal{A}) = 1$ if $\boldsymbol{x} \in \mathcal{A}$ and zero otherwise.

IV. SYSTEM MODEL

Let us consider an asynchronous CDMA system with K users in the uplink channel. Each user and the base station are equipped with a single antenna. The channel is flat[2] fading and impaired by additive white Gaussian noise. Then, the signal received at the base station, in complex base-band notation, is given by

$$y(t) = \sum_{k=1}^{K} a_k s_k(t - \tau_k) + w(t) \qquad t \in (-\infty, +\infty). \tag{4}$$

Here, a_k is the received signal amplitude of user k, which takes into account the transmitted amplitude, the effects of the flat fading, and the carrier phase offset; τ_k is the time delay of user k; $w(t)$ is a zero mean white, complex Gaussian process with power spectral density N_0; and $s_k(t)$ is the spread signal of user k. We have

$$s_k(t) = \sum_{m=-\infty}^{+\infty} b_k[m] c_k^{(m)}(t), \tag{5}$$

where $b_k[m]$ is the m^{th} transmitted symbol of user k and

$$c_k^{(m)}(t) = \sum_{n=0}^{N-1} s_{k,m}[n] \psi(t - mT_s - nT_c) \tag{6}$$

is its spreading waveform at time m. Here, $\boldsymbol{s}_k^{(m)}$ is the spreading sequence vector of user k in the m^{th} symbol interval with elements $s_{k,m}[n]$, $n = 0, \ldots, N-1$. T_s and $T_c = \frac{T_s}{N}$ are the symbol and chip interval, respectively.

The users' symbols $b_k[m]$ are independent and identically distributed (i.i.d.) random variables with $\mathrm{E}\{|b_k[m]|^2\} = 1$ and $\mathrm{E}\{b_k[m]\} = 0$. The elements of the spreading sequences $s_k^{(m)}[n]$ are assumed to be i.i.d. random variables with $\mathrm{E}\{|s_{k,m}[n]|^2\} = \frac{1}{N}$ and $\mathrm{E}\{s_{k,m}[n]\} = 0$. This assumption properly models the spreading sequences of some CDMA systems currently in use, such as the long spreading codes of the FDD (Frequency Division Duplex) mode in the UMTS uplink channel.

The chip waveform $\psi(t)$ is limited to bandwidth B and energy $E_\psi = \int_{-\infty}^{+\infty} |\psi(t)|^2 \mathrm{d}t$. Because of the constraint on the variance of the chips, i.e. $\mathrm{E}\{|s_{k,m}[k]|^2\} = \frac{1}{N}$, the mean energy of the signature waveform satisfies $\mathrm{E}\left\{\int_{-\infty}^{+\infty} |c_k^{(m)}(t)|^2 \mathrm{d}t\right\} = E_\psi$. We assume

1) user 1 as reference user so that $\tau_1 = 0$,
2) the users are ordered according to increasing time delay with respect to the reference user,

[2]Flat fading is no restriction of generality here as long as the excess delay is much smaller than the symbol interval T_s. This is, as the effect of multi-path can be incorporated into the shape of the chip waveform.

3) the time delay to be, at most, one chip interval so that $\tau_k \in [0, T_c)$.

Assumptions 1 and 2 are without loss of generality [29]. Assumption 3 is made for the sake of clarity and it will be removed in Section VII where the results are extended to the general case with $\tau_k \in [0, T_s)$.

At the receiver front-end, the base band signal is passed through a filter with impulse response $g(t)$ and corresponding transfer function $G(\omega)$ normalized such that $\int_{-\infty}^{+\infty} |g(t)|^2 \mathrm{d}t = 1$. We denote by $\phi(t)$ the response of the filter to the input $\psi(t)$, i.e. $\phi(t) = g(t) * \psi(t)$ and by $\Phi(\omega)$ its Fourier transform. The filter output is sampled at rate $\frac{r}{T_c}$ with $r \in \mathbb{N}$. For further convenience, we also define $E_\phi = \int_{-\infty}^{+\infty} |\phi(t)|^2 \mathrm{d}t$.

Throughout this work we assume that the filtered chip pulse waveform $\phi(t)$ is much shorter than the symbol waveform, i.e. $\phi(t)$ becomes negligible for $|t| > t_0$ and $t_0 \ll T_s$. This technical assumption is usually verified in the systems with large spreading factor we are considering. It allows to neglect intersymbol interference. Thus, focusing on a given symbol interval, we can omit the symbol index m and the discrete-time signal at the front-end output is given by

$$y[p] = \sum_{k=1}^{K} a_k b_k \overline{c}_k \left(\frac{p}{r} T_c - \tau_k \right) + w[p] \tag{7}$$

with sampling time $p \in \{0, \ldots, rN-1\}$ and

$$\overline{c}_k = \sum_{n=0}^{N-1} s_k[n] \phi \left(t - nT_c \right). \tag{8}$$

Here, $w[p]$ is discrete-time, complex-valued noise. In general, $w[p]$ is not white, although the continuous process was white. However, it *is* white, if $g(t) * g(-t)$ is Nyquist with respect to the sampling rate.

In order to cope with the effects of oversampling, we consider an extended signal space with virtual spreading sequences of length rN. The virtual spreading sequence of user k is given by the Nr-dimensional vector

$$\overline{\boldsymbol{\Phi}}_k \boldsymbol{s}_k \tag{9}$$

where $\boldsymbol{s}_k = (s_k[0] \ldots s_k[N-1])^T$,

$$\overline{\boldsymbol{\Phi}}_k = \begin{pmatrix} \boldsymbol{\phi}_{-\tau_k} & \boldsymbol{\phi}_{-T_c-\tau_k} & \cdots & \boldsymbol{\phi}_{(-N+1)T_c-\tau_k} \\ \boldsymbol{\phi}_{T_c-\tau_k} & \boldsymbol{\phi}_{-\tau_k} & \cdots & \boldsymbol{\phi}_{(-N+2)T_c-\tau_k} \\ \vdots & \vdots & \vdots & \vdots \\ \boldsymbol{\phi}_{(N-1)T_c-\tau_k} & \boldsymbol{\phi}_{(N-2)T_c-\tau_k} & \cdots & \boldsymbol{\phi}_{-\tau_k} \end{pmatrix} \tag{10}$$

is a $Nr \times N$ block matrix taking into account the effects of delay and pulse shaping. Its blocks are the vectors $\boldsymbol{\phi}_x = \left(\phi(x), \phi\left(x + \frac{T_c}{r}\right), \ldots, \phi\left(x + \frac{r-1}{r}T_c\right)\right)^T$. In that way, we have described user k's continuous-time channel with continuous delays canonically by the discrete-time channel matrix $\overline{\boldsymbol{\Phi}}_k$. Note that $\overline{\boldsymbol{\Phi}}_k$ solely depends on the delay of user k, the oversampling factor r, the chip waveform, and the receive filter.

Structuring the matrix $\overline{\boldsymbol{\Phi}}_k$ in blocks of dimensions $r \times 1$, it is block-wise Toeplitz. As well known [30], [31], block-Toeplitz and block-circulant matrices are asymptotically equivalent in terms of spectral distribution. This asymptotic equivalence is sufficient for us, since our only concern in this work are performance measures of CDMA systems which depend only on the asymptotic eigenvalue distribution. Similar asymptotically tight approximations are used in the large system analysis of CDMA in frequency-selective fading [32], [33], [34].

The equivalent block-circulant matrix is given by

$$\boldsymbol{\Phi}_k = \mathfrak{F}\left\{\left[\phi(\Omega, \tau_k), \phi\left(\Omega, \tau_k - \tfrac{T_c}{r}\right), \ldots, \phi\left(\Omega, \tau_k - \tfrac{(r-1)T_c}{r}\right)\right]\right\}, \tag{11}$$

where

$$\phi(\Omega, \tau) \stackrel{\triangle}{=} \frac{1}{T_c} \sum_{\nu=-\infty}^{+\infty} \mathrm{e}^{j\frac{\tau}{T_c}(\Omega + 2\pi\nu)} \Phi^*\left(\tfrac{1}{T_c}(\Omega + 2\pi\nu)\right) \tag{12}$$

is the spectrum of the chip waveform $\phi(t)$ delayed by τ and sampled at rate $1/T_c$. Thus, we replace the block-Toeplitz matrix $\overline{\boldsymbol{\Phi}}_k$ for our asymptotic analysis by the block-circulant matrix $\boldsymbol{\Phi}_k$ in the following and use the virtual spreading sequences

$$\boldsymbol{v}_k = \boldsymbol{\Phi}_k \boldsymbol{s}_k. \tag{13}$$

Let $\boldsymbol{S}$ be the $rN \times K$ matrix of virtual spreading, i.e. $\boldsymbol{S} = (\boldsymbol{\Phi}_1\boldsymbol{s}_1, \boldsymbol{\Phi}_2\boldsymbol{s}_2, \ldots \boldsymbol{\Phi}_K\boldsymbol{s}_K)$, $\boldsymbol{A}$ the $K \times K$ diagonal matrix of received amplitudes, $\boldsymbol{H} = \boldsymbol{S}\boldsymbol{A}$, and $\boldsymbol{b}$ and

$$\boldsymbol{y} = \boldsymbol{H}\boldsymbol{b} + \boldsymbol{w} \tag{14}$$

the vectors of transmitted and received signals, respectively. Additionally, $\boldsymbol{h}_k$ denotes the k^{th} column of the matrix $\boldsymbol{H}$. Finally, we define the correlation matrices $\boldsymbol{T} = \boldsymbol{H}\boldsymbol{H}^H$, $\boldsymbol{R} = \boldsymbol{H}^H\boldsymbol{H}$ and the system load $\beta = \frac{K}{N}$.

V. LINEAR MMSE DETECTION

The linear MMSE detector $\boldsymbol{d}_k$ generates a soft decision $\widehat{b}_k = \boldsymbol{d}_k^H\boldsymbol{y}$ of the transmitted symbol b_k based on the observation $\boldsymbol{y}$. It can be derived from the Wiener-Hopf theorem [35] and is given by

$$\boldsymbol{d}_k = \mathrm{E}\{\boldsymbol{y}\boldsymbol{y}^H\}^{-1}\mathrm{E}\{b_k^*\boldsymbol{y}\} \tag{15}$$

with the expectation taken over the transmitted symbols $\boldsymbol{b}$ and the noise. Specializing the Wiener-Hopf equation to the system model (14) yields

$$\boldsymbol{d}_k = (\boldsymbol{H}\boldsymbol{H}^H + \sigma^2\boldsymbol{I})^{-1}\boldsymbol{h}_k \tag{16}$$

$$= c \cdot (\boldsymbol{H}_k\boldsymbol{H}_k^H + \sigma^2\boldsymbol{I})^{-1}\boldsymbol{h}_k \tag{17}$$

for some $c \in \mathbb{R}$. Here, $\boldsymbol{H}_k$ is the matrix obtained from $\boldsymbol{H}$ suppressing column $\boldsymbol{h}_k$. The second step follows from the matrix inversion lemma.

The performance of the linear MMSE detector is measured by the signal-to-interference-and-noise ratio at its output [28]

$$\mathrm{SINR}_k = \boldsymbol{h}_k^H(\boldsymbol{H}_k\boldsymbol{H}_k^H + \sigma^2\boldsymbol{I})^{-1}\boldsymbol{h}_k. \tag{18}$$

The SINR can be conveniently expressed in terms of the multiuser efficiency η_k [28]

$$\mathrm{SINR}_k = \frac{|a_k|^2 E_\phi}{N_0}\,\eta_k. \tag{19}$$

The multiuser efficiency is a useful measure, since for large systems it is identical for all users in special cases [7] and it is related to the spectral efficiency [7], [36], [37].

The SINR depends on the spreading sequences, the received powers of all users, the chip pulse shaping, and the time delays of all users. To get deeper insight on the linear MMSE detector it is convenient to analyze the performance for random spreading sequences in the large system limits, i.e. as $K, N \to \infty$ with the ratio $\frac{K}{N} \to \beta$ kept fixed. The large-system analysis will identify the macroscopic parameters that characterize a chip-asynchronous CDMA system and the influences of chip pulse shaping and delay distribution.

In this section we present the large system analysis of a linear MMSE detector for chip-asynchronous CDMA systems with random spreading. Provided that the noise at the output of the front end is white, the analysis applies to CDMA systems using either optimum or suboptimum statistics, any chip pulse waveforms, and any set of time delays in $[0, T_c)$ if their empirical distribution function converges to a deterministic limit.

In Appendix II, we derive the following theorem on the large-system performance of chip-asynchronous CDMA:

Theorem 1 *Let $\boldsymbol{A} \in \mathbb{C}^{K\times K}$ be a diagonal matrix with k^{th} diagonal element $a_k \in \mathbb{C}$ and T_c a positive real. Given a function $\Phi(\omega) : \mathbb{R} \to \mathbb{C}$, let $\phi(\Omega, \tau)$ be as in (12). Given a positive integer r, let $\boldsymbol{\Phi}_k$,*

$k = 1, \ldots, K$, be r-block-wise circulant matrices of order N defined in (11). Let $\boldsymbol{H} = \boldsymbol{S}\boldsymbol{A}$ with $\boldsymbol{S} = [\boldsymbol{\Phi}_1\boldsymbol{s}_1, \boldsymbol{\Phi}_2\boldsymbol{s}_2, \ldots, \boldsymbol{\Phi}_K\boldsymbol{s}_K]$ and $\boldsymbol{s}_k \in \mathbb{C}^{N\times 1}$.

Assume that the function $|\Phi(\omega)|$ is upper bounded and has finite support. The receive filter is such that the sampled discrete-time noise process is white. The vectors $\boldsymbol{s}_k$ are independent with i.i.d. circularly symmetric Gaussian elements. Furthermore, the elements a_k of the matrix $\boldsymbol{A}$ are uniformly bounded for any K. The sequence of the empirical joint distributions $F^{(K)}_{|\boldsymbol{A}|^2,T}(\lambda,\tau) = \frac{1}{K}\sum_{k=1}^{K}\chi(\lambda > |a_k|^2)\chi(\tau > \tau_k)$ converges almost surely, as $K \to \infty$, to a non-random distribution function $F_{|\boldsymbol{A}|^2,T}(\lambda,\tau)$.

Then, given the received power $|a_k|^2$, the time delay τ_k and the variance of the white noise $\sigma^2 = \frac{rN_0}{T_c}$, the SINR of user k at the output of a linear MMSE detector for a CDMA system with transfer matrix $\boldsymbol{H}$ converges in probability as $K, N \to \infty$ with $\frac{K}{N} \to \beta$ and r fixed to

$$\lim_{K=\beta N\to\infty} \mathrm{SINR}_k = \frac{|a_k|^2}{2\pi}\int_{-\pi}^{\pi} \boldsymbol{\Delta}^H_{\phi,r}(\Omega,\tau_k)\boldsymbol{\Upsilon}(\Omega)\boldsymbol{\Delta}_{\phi,r}(\Omega,\tau_k)\mathrm{d}\Omega \tag{20}$$

where $\boldsymbol{\Upsilon}(\Omega)$ is the unique positive definite $r \times r$ matrix solution of the fixed point matrix equation[3]

$$\boldsymbol{\Upsilon}^{-1}(\Omega) = \sigma^2\boldsymbol{I}_r + \beta\int \frac{\lambda\boldsymbol{\Delta}_{\phi,r}(\Omega,\tau)\boldsymbol{\Delta}^H_{\phi,r}(\Omega,\tau)\mathrm{d}F_{|\boldsymbol{A}|^2,T}(\lambda,\tau)}{1+\frac{\lambda}{2\pi}\int_{-\pi}^{\pi}\boldsymbol{\Delta}^H_{\phi,r}(\Omega,\tau)\boldsymbol{\Upsilon}(\Omega)\boldsymbol{\Delta}_{\phi,r}(\Omega,\tau)\mathrm{d}\Omega} \qquad -\pi < \Omega \le \pi, \tag{21}$$

and

$$\boldsymbol{\Delta}_{\phi,r}(\Omega,\tau) = \begin{pmatrix} \phi(\Omega,\tau) \\ \phi(\Omega,\tau-\frac{T_c}{r}) \\ \vdots \\ \phi(\Omega,\tau-\frac{T_c(r-1)}{r}) \end{pmatrix}. \tag{22}$$

The performance of the linear MMSE detector operating on not necessarily sufficient statistics is completely characterized by

1) an $r \times r$ matrix-valued transfer function $\boldsymbol{\Upsilon}(\Omega)$ and
2) the frequency and delay dependent vector $\boldsymbol{\Delta}_{\phi,r}(\Omega,\tau)$

[3]Here, the integration measure is meant to denote $\mathrm{d}F_{|\boldsymbol{A}|^2,T}(\lambda,\tau) = f_{|\boldsymbol{A}|^2,T}(\lambda,\tau)\mathrm{d}\lambda\mathrm{d}\tau$ in case such a representation exists.

The multiuser efficiency varies from user to user and depends on the time delay of the user of interest only through $\mathbf{\Delta}_{\phi,r}(\Omega,\tau_k)$. We can define an SINR spectrum

$$\mathrm{SINR}_k(\Omega) = \frac{|a_k|^2}{2\pi}\mathbf{\Delta}_{\phi,r}^H(\Omega,\tau_k)\mathbf{\Upsilon}(\Omega)\mathbf{\Delta}_{\phi,r}(\Omega,\tau_k) \tag{23}$$

in the normalized frequency domain $-\pi < \Omega \leq \pi$, or, equivalently, a spectrum of the multiuser efficiency. The system performance is in both cases obtained by integration over the spectral components.

The fixed point equation (21) clearly reveals how and why synchronous users are the worst case for a given chip waveform. We know from [37] that to each large multiuser system, there is an equivalent single user system with enhanced noise, but otherwise identical performance. In the present case with oversampling factor r, the equivalent single user system is a frequency-selective MIMO (multiple-input multiple-output) system with r transmit and r receive antenna and governed by the $r \times r$ channel transfer matrix

$$\beta \int \frac{\lambda \mathbf{\Delta}_{\phi,r}(\Omega,\tau)\mathbf{\Delta}_{\phi,r}^H(\Omega,\tau)\mathrm{d}F_{|\boldsymbol{A}|^2,T}(\lambda,\tau)}{1+\frac{\lambda}{2\pi}\int_{-\pi}^{\pi}\mathbf{\Delta}_{\phi,r}^H(\Omega,\tau)\mathbf{\Upsilon}(\Omega)\mathbf{\Delta}_{\phi,r}(\Omega,\tau)\mathrm{d}\Omega}. \tag{24}$$

Note that this matrix is an integral of an outer product over the delay distribution. Thus, for constant delay, i.e. chip-synchronization, the matrix has rank one. No additional dimensions in signal space can be spanned. For distributed delays, the rank of the matrix can be as large as the oversampling factor r. Driving the equivalence even further, the equivalent MIMO system can be transformed into an equivalent CDMA system with spreading factor r and spreading sequences $\mathbf{\Delta}_{\phi,r}(\Omega,\tau_k)$. In this model, equal delays in the real CDMA system correspond to users with identical signature sequences in the equivalent CDMA system.

One cannot increase performance unboundedly by faster oversampling, as not all modes of the equivalent r-dimensional MIMO system can be excited with a chip waveform of limited excess bandwidth due to the projection onto the spectral support of the chip waveform in (20). In order to utilize the excess bandwidth of the system, we need two ingredients: 1) Time delays separating the users by making the signatures in the equivalent system differ. 2) A receiver that transforms the continuous-time receive signal into sufficient discrete-time statistics, e.g. by oversampling. A lack of different delays leads to a system where only a single eigenmode of the equivalent MIMO system is excited. A lack of oversampling leads to a system where more eigenmodes are excited, but are not converted into discrete time.

Additional intuitive insight into the behavior of the asynchronus CDMA systems can be gained by focusing on CDMA systems with uniformly distributed delay. In this case, Theorem 1 can be formulated with a single scalar fixed point equation by moving from the frequency Ω that is normalized to the chip rate to the unnormalized frequency ω. This yields the following corollary:

Corollary 2 *Let us adopt the same definitions as in Theorem 1 and let the assumptions of Theorem 1 be satisfied. Additionally, assume that the random variables λ and τ in $F_{|\boldsymbol{A}|^2,T}(\lambda,\tau)$ are statistically independent and the random variable τ is uniformly distributed in $[0,T_c)$. Furthermore, let $\Phi(\omega)$ vanish outside the interval $[-2\pi B;+2\pi B]$ with $B \leq \frac{r}{2T_c}$. Then, the multiuser efficiency of the linear MMSE detector for CDMA converges in probability as $K,N \to \infty$ with $\frac{K}{N} \to \beta$ and r fixed to*

$$\lim_{K=\beta N\to\infty} \eta_k = \eta = \frac{1}{2\pi} \int_{-2\pi B}^{+2\pi B} \eta\left(\omega\right) \mathrm{d}\omega \tag{25}$$

where the multiuser efficiency spectral density $\eta\left(\omega\right)$ is the unique solution to the fixed point equation

$$\frac{1}{\eta\left(\omega\right)} = \frac{E_\phi}{|\Phi\left(\omega\right)|^2} + \frac{\beta}{T_c} \int \frac{\lambda \mathrm{d}F_{|\boldsymbol{A}|^2}(\lambda)}{\frac{N_0}{E_\phi} + \lambda\eta} \tag{26}$$

and is zero for $|\omega| > 2\pi B$.

Theorem 1 is specialized to Corollary 2 in Appendix III.

Under the conditions of Corollary 2 the multiuser efficiency of the linear MMSE detector in asynchronous systems is the same for all users.

Rewriting (25) and (26) in terms of SINRs, these equations can be interpreted similarly to the corresponding equations in [5] for synchronous systems when the concept of effective interference is generalized to the concept of effective interference spectral density. Let $P(\omega,\lambda) = \frac{\lambda}{T_c}\left|\Phi\left(\omega\right)\right|^2$ be the power spectral density of the received signal for a user having received power λ. Then, the result in Corollary 2 can be expressed as

$$\mathrm{SINR}_k = \frac{1}{2\pi} \int_{-2\pi B}^{+2\pi B} \mathrm{sinr}_k(\omega)\mathrm{d}\omega \tag{27}$$

where the SINR spectral density $\mathrm{sinr}_k(\omega)$ is given by

$$\mathrm{sinr}_k(\omega) = \frac{P(\omega,|a_k|^2)}{N_0 + \beta \mathrm{E}_\lambda\{I(P(\omega,|a_k|^2),P(\omega,\lambda),\mathrm{SINR}_k)\}} \tag{28}$$

with the effective interference spectral density

$$I(P(\omega,|a_k|^2),P(\omega,\lambda),\mathrm{SINR}_k) = \frac{P(\omega,|a_k|^2)P(\omega,\lambda)}{P(\omega,|a_k|^2) + P(\omega,\lambda)\mathrm{SINR}_k}. \tag{29}$$

Heuristically, this means that for large systems the SINR spectral density is deterministic and given by

$$\mathrm{sinr}_k(\omega) \approx \frac{P(\omega,|a_k|^2)}{N_0 + \frac{1}{N}\sum_{j\neq k} I(P(\omega,|a_k|^2),P(\omega,|a_j|^2),\mathrm{SINR}_k)}. \tag{30}$$

This result yields an interpretation of the effects of each of the interfering users on the SINR of user k similar to the case of synchronous systems in [5]. The impairment at frequency ω can be decoupled into a sum of the background noise and an interference term from each of the users at the same frequency. The cumulated interference spectral density at frequency ω depends only on the received power density of the user of interest at this frequency, the received power spectral density of the interfering users at this frequency, and the attained SINR of user k. In other words, in asynchronous systems we have a decoupling of the effects of interferers like in synchronous systems and an additional decoupling in frequency. The term $I(P(\omega,|a_k|^2),P(\omega,|a_j|^2),\mathrm{SINR}_k)$ is the effective interference spectral density of user j onto user k at frequency ω for a given SINR of user k.

Sinc waveforms have a particular theoretical interest. In the following we specialize Corollary 2 to this case.

Corollary 3 *Let us adopt the definitions in Theorem 1 and let the assumptions of Corollary 2 be satisfied. Given a positive real α, we assume that*

$$\Phi(\omega)=\begin{cases}\sqrt{\frac{T_c}{\alpha}} & \text{for} \quad |\frac{\omega}{2\pi}|\leq\frac{\alpha}{2T_c},\\ 0 & \text{otherwise.}\end{cases} \tag{31}$$

corresponding to a sinc waveform with bandwidth $B=\frac{\alpha}{2T_c}$ and unit energy. Then, the multiuser efficiency of the linear MMSE detector converges in probability as $K,N\to\infty$ with $\frac{K}{N}\to\beta$ to

$$\lim_{K=\beta N\to\infty}\eta_k=\eta_{\mathrm{sinc}} \tag{32}$$

where the multiuser efficiency η_{sinc} is the unique positive solution to the fixed point equation

$$\frac{1}{\eta_{\mathrm{sinc}}}=1+\frac{\beta}{\alpha}\int\frac{\lambda\mathrm{d}F_{|\boldsymbol{A}|^2}(\lambda)}{N_0+\lambda\eta_{\mathrm{sinc}}}. \tag{33}$$

We recall that the multiuser efficiency of a linear MMSE detector for a synchronous CDMA system satisfies [5]

$$\frac{1}{\eta_{\mathrm{syn}}}=1+\beta\int\frac{\lambda\mathrm{d}F_{|\boldsymbol{A}|^2}(\lambda)}{N_0+\lambda\eta_{\mathrm{syn}}}. \tag{34}$$

This result holds for synchronous CDMA systems using any chip pulse waveform with bandwidth $B\geq\frac{1}{2T_c}$ and satisfying the Nyquist criterion. Thus, it also applies to sinc pulses whose bandwidth is an integer

multiple of $\frac{1}{2T_c}$. Then, Corollary 3 shows the interesting effect that an asynchronous CDMA system using a sinc function with bandwidth $B = \frac{\alpha}{2T_c}$ as chip pulse waveform performs as well as a synchronous CDMA system with bandwidth $\frac{r}{2T_c}, r \in \mathbb{N}$, with system load $\beta' = \frac{\beta}{\alpha}$. This implies that only asynchronous CDMA has the capability to trade the excess bandwidth of the chip pulse waveform against the spreading factor while synchronous CDMA has not. In other words, asynchronous CDMA offers to trade degrees of freedom in the frequency domain provided by the excess bandwidth of the chip pulse waveform against degrees of freedom in the time domain provided by spreading.

This phenomenon is similar to the resource pooling in CDMA systems with spatial diversity discovered in [38]. There, the degrees of freedom in space provided by multiple antennas at the receiver could be traded against degrees of freedom in time provided by the spreading. In order to make resource pooling happen, it is necessary that the steering vectors of the antenna arrays point into different directions. This condition is equivalent to requiring de-synchronization among users. If all users experience the same delay, this is like having totally correlated antenna elements.

In Corollary 3, the bandwidth of the sinc waveform may be either larger or smaller than the Nyquist bandwidth. For larger bandwidth, we get a resource pooling effect, for smaller bandwidth we create inter-chip interference and what could be called *anti-resource pooling*. Inter-chip interference is no particular cause of concern. In contrast, the effect of anti-resource pooling is to virtually increase the load, i.e. squeezing the same number of data into a smaller spectrum or equivalently squeezing more users into the same spectrum. Since spectral efficiency of optimum joint decoding is an increasing function of the load [4], anti-resource pooling is beneficial for spectral efficiency, though its implementation may cause some practical challenges.

In the following theorem, we extend anti-resource pooling to arbitrary delay distributions:

Theorem 2 *Let $\boldsymbol{A} \in \mathbb{C}^{K\times K}$ be a diagonal matrix with k^{th} diagonal element $a_k \in \mathbb{C}$ and T_c a positive real. Given a function $\Phi(\omega) : \mathbb{R} \to \mathbb{C}$, let $\phi(\Omega, \tau)$ be as in (12). Given a positive integer r, let $\boldsymbol{\Phi}_k$, $k = 1, \ldots, K$, be r-block-wise circulant matrices of order N defined in (11). Let $\boldsymbol{H} = \boldsymbol{S}\boldsymbol{A}$ with $\boldsymbol{S} = [\boldsymbol{\Phi}_1\boldsymbol{s}_1, \boldsymbol{\Phi}_2\boldsymbol{s}_2, \ldots, \boldsymbol{\Phi}_K\boldsymbol{s}_K]$ and $\boldsymbol{s}_k \in \mathbb{C}^{N\times 1}$.*

Assume that the function $|\Phi(\omega)|$ is upper bounded and has support contained in the interval $\left[-\frac{\pi}{T_c}, \frac{\pi}{T_c}\right]$. The receive filter is such that the sampled discrete-time noise process is white. The vectors $\boldsymbol{s}_k$ are independent with i.i.d. circularly symmetric Gaussian elements. Furthermore, the elements a_k of the matrix $\boldsymbol{A}$ are

uniformly bounded for any K. The sequence of the empirical distributions $F^{(K)}_{|\boldsymbol{A}|^2}(\lambda) = \frac{1}{K}\sum_{k=1}^{K}\chi(\lambda \leq |a_k|^2)$ converges in law almost surely, as $K \to \infty$, to a non-random distribution function $F_{|\boldsymbol{A}|^2}(\lambda)$.

Then, the multiuser efficiency of the linear MMSE detector for CDMA with transfer matrix $\boldsymbol{H}$ converges in probability as $K, N \to \infty$ with $\frac{K}{N} \to \beta$ and r fixed to

$$\lim_{K=\beta N\to\infty} \eta_k = \eta = \frac{1}{2\pi}\int_{-\pi/T_c}^{+\pi/T_c} \eta\left(\omega\right) \mathrm{d}\omega \tag{35}$$

where the multiuser efficiency spectral density $\eta(\omega)$ is the unique solution to the fixed point equation

$$\frac{1}{\eta\left(\omega\right)} = \frac{E_\phi}{|\Phi(\omega)|^2} + \frac{\beta}{T_c}\int \frac{\lambda \mathrm{d}F_{|\boldsymbol{A}|^2}(\lambda)}{\frac{N_0}{E_\phi} + \lambda\eta} \tag{36}$$

for all ω in the support of $\Phi(\omega)$ and zero elsewhere.

Theorem 2 is proven in Appendix IV.

No constraint is imposed on the set of time delays in Theorem 2. It holds for any set $\{\tau_1, \tau_2 \ldots \tau_K\}$ and we conclude that linear MMSE detectors for synchronous and asynchronous CDMA systems have the same performance if the bandwidth of the chip pulse waveforms satisfies the constraint $B \leq \frac{1}{2T_c}$.

VI. SPECTRAL EFFICIENCY

There exists a close relation between the total capacity of a CDMA system and the multiuser efficiency of a linear MMSE detector for the same system [7], [36], [37]. The rationale behind this relation is a fundamental connection between mutual information and minimum mean-squared error in Gaussian channels [39]. In the following, we extend the results in Section V to get insight into the spectral efficiency of an asynchronous CDMA system.

The capacity of the CDMA channel was found in [40] for synchronous CDMA systems. The total capacity per chip for large synchronous CDMA systems with square root Nyquist pulses and random spreading in the presence of AWGN (additive white Gaussian noise) is [4]

$$\begin{aligned}\mathcal{C}^{(\text{syn})}(\beta, \text{SNR}) = \beta\log_2\left(1 + \text{SNR} - \frac{1}{4}\mathcal{F}\left(\text{SNR}, \beta\right)\right) + \log_2\left(1 + \beta\text{SNR} - \frac{1}{4}\mathcal{F}\left(\text{SNR}, \beta\right)\right) \\ - \frac{\log_2 e}{4\,\text{SNR}}\,\mathcal{F}\left(\text{SNR}, \beta\right)\end{aligned} \tag{37}$$

with

$$\digamma(y,z) = \left(\sqrt{y(1+\sqrt{z})^2+1} - \sqrt{y(1-\sqrt{z})^2+1}\right)^2. \tag{38}$$

With the normalizations adopted in the system model, we have $\mathrm{SNR} = E_\phi/N_0$.

The spectral efficiency of a synchronous CDMA system is equal to $\mathcal{C}^{(\mathrm{syn})}(\beta, \mathrm{SNR})$ for any Nyquist sinc waveform. For other chip waveforms, we need to take into account the excess bandwidth and calculate spectral efficiency as

$$\Gamma = \frac{\mathcal{C}}{T_c B} \tag{39}$$

where $\mathcal{C}$ denotes the total capacity per chip and B denotes the bandwidth of the chip pulse. Note that for Nyquist sinc pulses $T_c B = 1$, while in general $T_c B$ can be either larger, e.g. for root-raised cosine pulses, or smaller, i.e. for anti-resource pooling, than 1.

The expression of the total capacity per chip for asynchronous CDMA systems constrained to a given chip pulse waveform $\psi(t)$ of bandwidth B and a given receive filter $g(t)$ can be obtained by making use of the results in Section V and the fundamental relation between mutual information and MMSE in Gaussian channels provided in [39]. Since such constrained total capacity depends on $\psi(t)$ and $g(t)$ only via the waveform $\phi(t)$, output of the filter $g(t)$ for the input $\psi(t)$, we shortly refer to it as the total capacity constrained to the chip waveform $\phi(t)$.

Corollary 4 *Let us adopt the same definitions as in Theorem 2 and let the assumptions of Corollary 2 or Theorem 2 be satisfied. Additionally, let the receive filter and sampling process be such that sufficient discrete-time statistics are provided. Then, as $K, N \to \infty$ with $\frac{K}{N} \to \beta$ the total capacity per chip constrained to the chip pulse waveform $\phi(t)$ converges to the deterministic value*

$$\mathcal{C}^{(\mathrm{asyn})}\left(\beta, \frac{E_\phi}{N_0}, \phi\right) = \frac{\beta}{\ln 2} \int_0^{\frac{E_\phi}{N_0}} \int \frac{\lambda \eta_\gamma \mathrm{d}F_{|\boldsymbol{A}|^2}(\lambda)}{1+\lambda\gamma\eta_\gamma}\,\mathrm{d}\gamma \tag{40}$$

where η_γ is the multiuser efficiency at signal-to-noise ratio γ given in (25) and (35), respectively.

The proof of this corollary is discussed in Appendix VI.

Let us consider again the case of sinc chip waveforms as defined in (31) and uniform distribution of the time delays. Let α denote the bandwidth of the since pulse relative to the Nyquist bandwidth. As noticed in Section V, the multiuser efficiency η_{sinc} of an asynchronous system with such sinc waveforms given by (33)

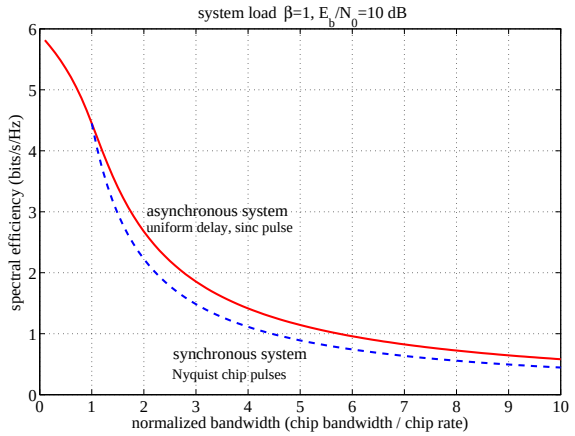

Fig. 1. Spectral efficiency of random CDMA with unit load versus the normalized bandwidth α and $\frac{E_b}{N_0} = 10$ dB.

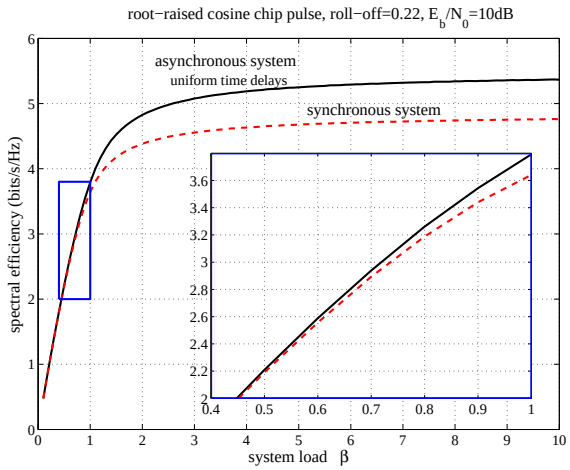

Fig. 2. Spectral efficiency of random CDMA versus the load β for the root-raised cosine chip pulse used in the UMTS standard and $\frac{E_b}{N_0} = 10$ dB.

and load β equals the multiuser efficiency η_{syn} of a synchronous system with Nyquist sinc pulses given by (34) and load $\beta' = \frac{\beta}{\alpha}$. Since the load enters capacity per chip (40) only via the multiuser efficiency except for the linear pre-factor to the integral, we immediately find the following equation relating the two capacities per chip

$$\mathcal{C}^{(\text{sinc})}(\beta, \text{SNR}, \alpha) = \alpha\, \mathcal{C}^{(\text{syn})}\left(\frac{\beta}{\alpha}, \text{SNR}\right). \tag{41}$$

It is apparent from (41) that synchronous and asynchronous systems have the same capacity for $\alpha = 1$.

In order to compare different systems (with possibly different spreading gains and data rates), spectral efficiency has to be given as a function of $\frac{E_b}{N_0}$, the level of energy per bit per noise level equal to [4] [7]

$$\frac{E_b}{N_0} = \frac{\beta \text{SNR}}{\mathcal{C}^{(*)}(\beta, \text{SNR}, \cdot)}. \tag{42}$$

In Figure 1, we compare the spectral efficiency of asynchronous CDMA with the spectral efficiency of synchronous CDMA. The spectral efficiencies are plotted against the bandwidth normalized to the Nyquist bandwidth with $\frac{E_b}{N_0} = 10\,\text{dB}$ and unit load $\beta = 1$. Recall from earlier discussions that for synchronous systems all Nyquist chip waveforms perform identically. So there is no need to specify a particular Nyquist pulse except for the Nyquist pulse having the same bandwidth than the sinc pulse in the asynchronous case. We see further that the smaller the normalized bandwidth, the higher the spectral efficiency is. This is, as anti-resource pooling improves spectral efficiency by emulating a higher load.

In Figure 2 the spectral efficiency is plotted against the load β with $\frac{E_b}{N_0} = 10\,\text{dB}$ for the chip waveform

used in the UMTS standard. When the load β increases the gap in spectral efficiency between synchronous and asynchronous systems increases.

VII. EXTENSION TO GENERAL ASYNCHRONOUS CDMA SYSTEMS

In this section we extend the previous results to any distribution of the time delays for CDMA systems. Without loss of generality we can assume that the time delays $\tau_k \in [0, T_s)$ [28]. In this case, intersymbol interference is not negligible and an infinite observation window is necessary to obtain sufficient statistics. Equation (14) for the chip asynchronous but symbol asynchronous system model is extended to a general asynchronous system by

$$y[p] = \sum_{k=1}^{K} a_k \sum_{m=-\infty}^{+\infty} b_k[m] \overline{c}_k^{(m)} \left(\frac{p}{r} T_c - \tau_k \right) + w[p] \tag{43}$$

with $p \in \mathbb{Z}$ and

$$\overline{c}_k^{(m)} = \sum_{u=0}^{N-1} s_{k,m}[u] \phi(t - (u+mN)T_c) \, . \tag{44}$$

By assuming the same approximation as in (14), the virtual spreading sequence of user k in the symbol interval m has nonzero elements only in the time interval m and $m+1$. Let $\overline{\tau}_k$ denote the delay of the signal k in terms of the chip intervals and $\widetilde{\tau}_k$ the delay within a chip, i.e. $\overline{\tau}_k = \left\lfloor \frac{\tau_k}{T_c} \right\rfloor$ and $\widetilde{\tau}_k = \tau_k \mathrm{mod} T_c$ respectively. The virtual spreading sequence of user k is obtained by computing $\mathbf{\Phi}_k$ as in (11) for $\tau = \widetilde{\tau}_k$ to account for the delay within a chip and then by shifting the virtual spreading vector down by $\overline{\tau}_k$ r-dimensional blocks to account for the delay multiple of the chip interval. More precisely, the virtual spreading in the m-th symbol interval is given by the $2rN$-dimensional vector

$$\begin{bmatrix} \mathbf{0}_{\overline{\tau}_k} \\ \mathfrak{F}(\boldsymbol{c}(\widetilde{\tau}_k) \\ \mathbf{0}_{N-\overline{\tau}_k} \end{bmatrix} \boldsymbol{s}_k^{(m)} = \widetilde{\mathbf{\Phi}}_k \boldsymbol{s}_k^{(m)} \tag{45}$$

with

$$\boldsymbol{c}(\widetilde{\tau}_k) = \left[\Phi(\Omega, \widetilde{\tau}_k), \Phi\left(\Omega, \widetilde{\tau}_k - \frac{T_c}{r}\right), \ldots \Phi\left(\Omega, \widetilde{\tau}_k - \frac{(r-1)T_c}{r}\right) \right],$$

$\mathbf{0}_{\overline{\tau}_k}$ and $\mathbf{0}_{N-\overline{\tau}_k}$ column vectors with zero entries and dimension $r\overline{\tau}_k$ and $r(N - \overline{\tau}_k)$, respectively. The $2rN \times K$ virtual spreading matrix for the symbols transmitted at time interval m is then

$$\widetilde{\boldsymbol{S}}^{(m)} = \left[\widetilde{\mathbf{\Phi}}_1 \boldsymbol{s}_1^{(m)}, \widetilde{\mathbf{\Phi}}_2 \boldsymbol{s}_2^{(m)}, \ldots \widetilde{\mathbf{\Phi}}_K \boldsymbol{s}_K^{(m)} \right].$$

For further study, we introduce the upper and lower part of the matrix $\widetilde{\boldsymbol{S}}^{(m)}$, $\widetilde{\boldsymbol{S}}_u^{(m)}$ and $\widetilde{\boldsymbol{S}}_d^{(m)}$ of size $rN \times rK$ such that

$$\widetilde{\boldsymbol{S}}^{(m)} = \begin{bmatrix} \widetilde{\boldsymbol{S}}_u^{(m)} \\ \widetilde{\boldsymbol{S}}_d^{(m)} \end{bmatrix}.$$

and the matrices $\widetilde{\boldsymbol{H}}_u^{(m)} = \widetilde{\boldsymbol{S}}_u^{(m)}\boldsymbol{A}$ and $\widetilde{\boldsymbol{H}}_d^{(m)} = \widetilde{\boldsymbol{S}}_d^{(m)}\boldsymbol{A}$. Then, the baseband discrete-time asynchronous system in matrix notation is given by

$$\boldsymbol{\mathcal{Y}} = \boldsymbol{\mathcal{H}}\boldsymbol{\mathcal{B}} + \boldsymbol{\mathcal{W}} \tag{46}$$

where $\boldsymbol{\mathcal{Y}} = [\ldots, \boldsymbol{y}^{(m-1)^T}, \boldsymbol{y}^{(m)^T}, \boldsymbol{y}^{(m+1)^T} \ldots]^T$ and $\boldsymbol{\mathcal{B}} = [\ldots, \boldsymbol{b}^{(m-1)^T}, \boldsymbol{b}^{(m)^T}, \boldsymbol{b}^{(m+1)^T} \ldots]^T$ are the infinite-length vectors of received and transmitted symbols respectively; $\boldsymbol{\mathcal{W}}$ is an infinite-length white Gaussian noise vector; and $\boldsymbol{\mathcal{H}}$ is a bi-diagonal block matrix with infinite block rows and block columns

$$\boldsymbol{\mathcal{H}} = \begin{bmatrix} \ddots & \ddots & \ddots & \ddots & \ddots & \ddots & \ddots \\ \ldots & \mathbf{0} & \widetilde{\boldsymbol{H}}_d^{(m-1)} & \widetilde{\boldsymbol{H}}_u^{(m)} & \mathbf{0} & \ldots & \ldots \\ \ldots & \ldots & \mathbf{0} & \widetilde{\boldsymbol{H}}_d^{(m)} & \widetilde{\boldsymbol{H}}_u^{(m+1)} & \mathbf{0} & \ldots \\ \ddots & \ddots & \ddots & \ddots & \ddots & \ddots & \ddots \end{bmatrix}. \tag{47}$$

Finally, we define the correlation matrices $\boldsymbol{\mathcal{T}} = \boldsymbol{\mathcal{H}}\boldsymbol{\mathcal{H}}^H$, $\boldsymbol{\mathcal{R}} = \boldsymbol{\mathcal{H}}^H\boldsymbol{\mathcal{H}}$.

The following theorem shows that a linear MMSE detector for a CDMA system with transfer matrix $\boldsymbol{\mathcal{H}}$ and time delays $\tau_1, \tau_2, \ldots \tau_K$ has the same limiting performance as a linear MMSE detector for chip asynchronous but symbol quasi-synchronous CDMA systems introduced in Section IV with time delays $\widetilde{\tau}_1, \widetilde{\tau}_2, \ldots \widetilde{\tau}_K$. The same equivalence holds for capacity and spectral efficiency.

Theorem 3 *Given $\{\tau_1, \tau_2, \ldots \tau_K\}$ a set of delays in $[0, T_s)$ let us consider the set of delays in $[0, T_c)$ defined as $\{\widetilde{\tau}_k : \widetilde{\tau}_k = \tau_k \mod T_c,\ k = 1, \ldots K\}$. Given a positive integer r, let $\boldsymbol{\Phi}_k$, $k = 1, \ldots K$, be the r-blockwise circulant matrix of order N defined in (11) with $\tau = \widetilde{\tau}_k$. Let $\boldsymbol{A}$, $\Phi(\omega)$, $\boldsymbol{S}$, and $\boldsymbol{H}$ be defined as in Theorem 1. Furthermore, $\widetilde{\boldsymbol{\Phi}}_k$, $k = 1 \ldots K$ are $2rN \times N$ matrices such that $\widetilde{\boldsymbol{\Phi}}_k = [\mathbf{0}_{\overline{\tau}_k}^T, \boldsymbol{\Phi}_k^T, \mathbf{0}_{N-\overline{\tau}_k}^T]^T$ with $\overline{\tau}_k = \left\lfloor \frac{\tau_k}{T_c} \right\rfloor$, $\mathbf{0}_{\overline{\tau}_k}$ and $\mathbf{0}_{N-\overline{\tau}_k}$ zero matrices of dimensions $r\overline{\tau_k} \times N$ and $r\,(N - \overline{\tau_k}) \times N$, respectively. Let $\widetilde{\boldsymbol{S}}^{(m)} = \left(\widetilde{\boldsymbol{\Phi}}_1 \boldsymbol{s}_1^{(m)}, \widetilde{\boldsymbol{\Phi}}_2 \boldsymbol{s}_2^{(m)} \ldots \widetilde{\boldsymbol{\Phi}}_K \boldsymbol{s}_K^{(m)}\right)$, $\widetilde{\boldsymbol{H}}^{(m)} = [\widetilde{\boldsymbol{H}}_u^{(m)T}, \widetilde{\boldsymbol{H}}_d^{(m)T}]^T = \widetilde{\boldsymbol{S}}\boldsymbol{A}$ and $\boldsymbol{\mathcal{H}}$ the infinite block row and block column matrix of the same form as in (47). Let the same assumptions as in Theorem 1 hold.*

Then, asymptotically, as $K, N \to \infty$ with $\frac{K}{N} \to \beta$ the CDMA systems transfer matrices $\boldsymbol{\mathcal{H}}$ and $\boldsymbol{H}$ are equivalent in terms of multiuser efficiency for linear MMSE detectors and in terms of spectral efficiency.

This theorem is shown in Appendix VII.

Interestingly, the system performance depends on the time delays τ_k only through the offsets $\widetilde{\tau}_k - \left\lfloor \frac{\tau_k}{T_c} \right\rfloor T_c$. Therefore, any shift of the signal multiple of T_c does not affect the performance of the system.

The analysis presented in this contribution has been restricted to frequency flat fading for the sake of clarity. The extension to multipath fading channels is straightforward when the impulse response of the channel is much shorter than the symbol interval. In fact, the chip pulse waveform at the output of the matched filter $\phi(t)$ can include the effects of the frequency selective channel impulse response $a(t)$ along with the effects of the transmitted chip pulse waveform $\psi(t)$, and the filter at the front-end $g(t)$, i.e. $\phi(t) = \psi(t) * a(t) * g(t)$. Then, the analysis of a system with frequency selective fading reduces to the proposed analysis.

VIII. CONCLUSIONS

This work provides a general framework for the analysis of asynchronous CDMA systems with random spreading using sufficient or suboptimum statistics and any chip pulse waveform. Furthermore, it includes several optimum or suboptimum receiver structures of practical and theoretical interest. Therefore, it provides insight into both the fundamental limits of asynchronous CDMA systems and the performance loss of implementations where suboptimum receiver structures, suboptimum statistics, and/or non-ideal chip pulses are utilized.

For the receiver structures investigated in Part I, the performance of a CDMA system is independent of the time delay distribution if the bandwidth of the chip pulse waveform is not greater than half of the chip rate, i.e. $B \leq \frac{1}{2T_c}$. This also implies that synchronous and asynchronous CDMA systems have the same performance and generalizes the equivalence result in [18] for Nyquist sinc ($B = \frac{1}{2T_c}$) pulses and linear MMSE detectors to any chip pulse waveform. The behavior of CDMA system changes substantially as the bandwidth gets larger. In this case, the system performance is significantly affected by the distribution of the time delays and the performance of linear detectors may depend on the specific time delay of the signal of interest. If the receiver is fed by sufficient statistics and the time delay distribution is uniform the performance of optimum or suboptimum receivers is independent of the time delays. In the following, we summarize the most interesting aspects pointed out by the large system analysis, for each class of receivers.

A. Optimum Receiver

The spectral efficiency constrained to a given chip pulse waveform characterizes the performance of a CDMA channel with optimum receiver. The spectral efficiency is expressed in terms of the multiuser efficiency spectral density $\eta(\omega)$. When the chip-modulation is based on sinc pulses whose bandwidth is α times the Nyquist bandwidth, the spectral efficiency of asynchronous CDMA systems is identical to the spectral efficiency of synchronous systems with load $\beta' = \frac{\beta}{\alpha}$ and Nyquist sinc pulses. Spectral efficiency is a strictly decreasing function of the relative pulse bandwidth α and for $\alpha \to 0$, the spectral efficiency of a single user AWGN channel is reached.

For $\alpha > 1$ an asynchronous CDMA system with modulation based on a sinc function can compensate to some extent for the loss in spectral efficiency of synchronous CDMA systems with equal bandwidth. For $\beta \to \infty$ it attains the maximum spectral efficiency for any finite bandwidth $B = \frac{\alpha}{2T_c}$.

B. Linear MMSE Detector

The output SINR of a linear MMSE detector can be obtained from the solution to a system of fixed point equations in the general case. In the two cases (i) chip pulses with bandwidth $B \leq \frac{1}{2T_c}$ and (ii) chip pulses with bandwidth $B > \frac{1}{2T_c}$, sufficient statistics and uniform time delay distribution the fixed point system of equation reduces to a single equation. In those cases, the performance of a linear MMSE detector in asynchronous CDMA systems is characterized by a unique value of multiuser efficiency. Furthermore, the measure of multiuser efficiency can be refined by the concept of spectrum of the multiuser efficiency that is also unique for all the users. Furthermore, for those CDMA systems the limiting interference effects, as the system grows large, can be decoupled into user domain and frequency domain such that we can define an effective interference spectral density similarly to the effective interference in [5] for synchronous systems.

In the special case that the modulation is based on sinc functions with bandwidth $B = \frac{\alpha}{2T_c}$ a linear MMSE detector in asynchronous CDMA channels performs identically to a synchronous CDMA system with square root Nyquist chip pulses [5] and load $\beta' = \frac{\beta}{\alpha}$. This effect is similar to the resource pooling effect for synchronous CDMA systems with spatial diversity in [38] and shows the possibility to trade degrees of freedom in the frequency domain against degrees of freedom in the time domain.

Though this work focused on performance measures for CDMA, similar results hold for asynchronous MIMO systems due to the mathematical analogy between CDMA and MIMO systems when described as a discrete-time vector channel. This means, that MIMO systems with excess bandwidth and desynchronized

modulators for different antenna elements benefit in a similar manner than CDMA systems with desynchronized users.

ACKNOWLEDGMENT

The authors thank Alex Grant and Dirk Slock for useful discussions.

APPENDIX I

USEFUL MATHEMATICAL TOOLS

Let $\Phi(\omega)$ be the unitary Fourier transform of a pulse waveform $\phi(t)$ with bandwidth $B \leq \frac{r}{2T_c}$. Then, in the normalized frequency interval $\Omega \in [-\pi, \pi]$ the unitary Fourier transform (12) of the sequence obtained by sampling $\phi(t)$ at time instant τ and rate $\frac{r}{T_c}$ is given by

$$\phi(\Omega,\tau) = \frac{1}{T_c} \mathrm{e}^{\frac{j\tau}{T_c}\Omega} \sum_{s=-\mathrm{sign}(\Omega)\left\lfloor \frac{r-1}{2} \right\rfloor}^{\mathrm{sign}(\Omega)\left\lfloor \frac{r}{2} \right\rfloor} \mathrm{e}^{j2\pi\frac{\tau}{T_c}s} \Phi^*\left(\frac{\Omega+2\pi s}{T_c}\right) \quad \text{for} \quad |\Omega| \leq \pi. \tag{48}$$

The matrix

$$\boldsymbol{Q}(\Omega,\tau) = \boldsymbol{\Delta}_{\phi,r}(\Omega,\tau)\boldsymbol{\Delta}_{\phi,r}(\Omega,\tau)^H, \tag{49}$$

with $\boldsymbol{\Delta}_{\phi,r}(\Omega,\tau)$ defined in (22), can be decomposed in the sum of two matrices

$$\boldsymbol{Q}(\Omega,\tau) = \boldsymbol{Q}(\Omega) + \overline{\boldsymbol{Q}}(\Omega,\tau) \tag{50}$$

where the (k,ℓ)-elements of the matrices $\boldsymbol{Q}(\Omega)$ and $\overline{\boldsymbol{Q}}(\Omega,\tau)$ are given by

$$(\boldsymbol{Q}(\Omega))_{k,\ell} = \frac{1}{T_c^2} \sum_{s=-\mathrm{sign}(\Omega)\left\lfloor \frac{r-1}{2} \right\rfloor}^{\mathrm{sign}(\Omega)\left\lfloor \frac{r}{2} \right\rfloor} \left|\Phi\left(\frac{\Omega+2\pi s}{T_c}\right)\right|^2 \mathrm{e}^{-j\frac{k-\ell}{r}(\Omega+2\pi s)} \quad \text{for} \quad |\Omega| \leq \pi, \tag{51}$$

and

$$(\overline{\boldsymbol{Q}}(\Omega,\tau))_{k,\ell} = \frac{1}{T_c^2} \sum_{\substack{s,u=-\mathrm{sign}(\Omega)\left\lfloor \frac{r-1}{2} \right\rfloor \\ s\neq u}}^{\mathrm{sign}(\Omega)\left\lfloor \frac{r}{2} \right\rfloor} \Phi\left(\frac{\Omega+2\pi u}{T_c}\right) \Phi^*\left(\frac{\Omega+2\pi s}{T_c}\right) \mathrm{e}^{-j2\pi\frac{\tau}{T_c}(s-u)} \mathrm{e}^{-j\left(\frac{k-1}{r}(\Omega-2\pi s)-\frac{\ell-1}{r}(\Omega-2\pi u)\right)}$$

$$\text{for} \quad |\Omega| \leq \pi, \tag{52}$$

respectively.

Useful properties of the matrices $\boldsymbol{Q}(\Omega)$ and $\overline{\boldsymbol{Q}}(\Omega,\tau)$ are stated in the following lemmas.

Lemma 1 *Let $\boldsymbol{B}$ be an $r \times r$ matrix of the form*

$$\boldsymbol{B} = \boldsymbol{B}(\Omega) = \begin{bmatrix} b_0 & b_1 \mathrm{e}^{j\frac{\Omega}{r}} & \dots & \dots & b_{r-1}\mathrm{e}^{j\frac{(r-1)}{r}\Omega} \\ b_{r-1}\mathrm{e}^{-j\frac{\Omega}{r}} & b_0 & b_1\mathrm{e}^{j\frac{\Omega}{r}} & \dots & b_{r-2}\mathrm{e}^{j\frac{(r-2)}{r}\Omega} \\ \dots & \ddots & \ddots & \ddots & \ddots \\ b_1\mathrm{e}^{-j\frac{(r-1)}{r}\Omega} & \ddots & \ddots & b_{r-1}\mathrm{e}^{-j\frac{\Omega}{r}} & b_0 \end{bmatrix}, \tag{53}$$

i.e. given $b_0 = b_0(\Omega), b_1 = b_1(\Omega), \dots b_{r-1} = b_{r-1}(\Omega)$, eventually functions of Ω, $(\boldsymbol{B})_{\ell,k}$, the element (ℓ, k) of the matrix $\boldsymbol{B}$ satisfies $(\boldsymbol{B})_{\ell,k} = \mathrm{e}^{\frac{j(k-\ell)}{r}\Omega} b_{(r+k-\ell)\mathrm{mod}r}$. Let $\overline{\boldsymbol{Q}}(\Omega,\tau)$ be the $r \times r$ matrix with element (k,ℓ) defined in (52). Then,

$$\mathrm{tr}(\boldsymbol{B}\overline{\boldsymbol{Q}}(\Omega,\tau)) = 0.$$

Proof: Let $\overline{q}_{us}(\Omega) = \frac{1}{T_c^2}\Phi\left(\frac{\Omega+2\pi u}{T_c}\right)\Phi^*\left(\frac{\Omega+2\pi s}{T_c}\right)$. Then,

$$\begin{aligned}
\mathrm{tr}(\boldsymbol{B}\overline{\boldsymbol{Q}}(\Omega+j2\pi u,\tau)) &= \sum_{k=1}^{r}\sum_{\ell=1}^{r}(\overline{\boldsymbol{Q}}(\Omega,\tau))_{k,\ell}(\boldsymbol{B})_{\ell,k} \\
&= \sum_{\substack{s,u=-\mathrm{sign}(\Omega)\left\lfloor\frac{r-1}{2}\right\rfloor \\ s\neq u}}^{\mathrm{sign}(\Omega)\left\lfloor\frac{r}{2}\right\rfloor} \overline{q}_{us}\mathrm{e}^{j2\pi\frac{\tau}{T_c}(s-u)}\sum_{k=1}^{r}\sum_{\ell=1}^{r}(\boldsymbol{B})_{\ell,k}\mathrm{e}^{-j\frac{k-\ell}{r}\Omega}\mathrm{e}^{-j\frac{2\pi}{r}(-s(k-1)+u(\ell-1))} \\
&= \sum_{\substack{s,u=-\mathrm{sign}(\Omega)\left\lfloor\frac{r-1}{2}\right\rfloor \\ s\neq u}}^{\mathrm{sign}(\Omega)\left\lfloor\frac{r}{2}\right\rfloor} \overline{q}_{us}\mathrm{e}^{j2\pi\left(\frac{\tau}{T_c}-\frac{1}{r}\right)(s-u)}\sum_{k=1}^{r}\sum_{\ell=1}^{r}b_{(r+k-\ell)\mathrm{mod}r}\mathrm{e}^{-j\frac{2\pi}{r}(u-s)k}\mathrm{e}^{j\frac{2\pi}{r}u(k-\ell)} \\
&= \sum_{\substack{s,u=-\mathrm{sign}(\Omega)\left\lfloor\frac{r-1}{2}\right\rfloor \\ s\neq u}}^{\mathrm{sign}(\Omega)\left\lfloor\frac{r}{2}\right\rfloor} \overline{q}_{us}\mathrm{e}^{j2\pi\left(\frac{\tau}{T_c}-\frac{1}{r}\right)(s-u)}(\eta_1+\eta_2)
\end{aligned}$$

with

$$\eta_1 = \sum_{\substack{k,\ell=1 \\ k\geq\ell}}^{r} b_{(r+k-\ell)\mathrm{mod}r}\mathrm{e}^{-j\frac{2\pi}{r}(u-s)k}\mathrm{e}^{j\frac{2\pi}{r}u(k-\ell)} \tag{54}$$

and

$$\eta_2 = \sum_{\substack{k,\ell=1 \\ k<\ell}}^{r} b_{(r+k-\ell)\mathrm{mod}r}\mathrm{e}^{-j\frac{2\pi}{r}(u-s)k}\mathrm{e}^{j\frac{2\pi}{r}u(k-\ell)}. \tag{55}$$

Substituting $v = k-\ell$ in (54) and $v = r+k-\ell$ in (55) we obtain

$$\eta_1 = \sum_{k=1}^{r}\sum_{v=0}^{k-1} b_v\mathrm{e}^{-j\frac{2\pi}{r}(u-s)k}\mathrm{e}^{j\frac{2\pi uv}{r}}$$

and

$$\eta_2 = \sum_{k=1}^{r}\sum_{v=k}^{r-1} b_v \mathrm{e}^{-j\frac{2\pi}{r}(u-s)k}\mathrm{e}^{j\frac{2\pi uv}{r}},$$

respectively. For $s,t \in [-\mathrm{sign}(\Omega)\left\lfloor\frac{r-1}{2}\right\rfloor \ldots 0 \ldots \mathrm{sign}(\Omega)\left\lfloor\frac{r}{2}\right\rfloor]$ and $s \neq t$, $|s-t| \in [1,\ldots,r-1]$. Therefore, $\sum_{k=1}^{r}\mathrm{e}^{-j\frac{2\pi}{r}(u-s)k} = 0$ and $\eta_1+\eta_2 = 0$ for all Ω. Then, also $\mathrm{tr}(\boldsymbol{B}\overline{\boldsymbol{Q}}(\Omega,\tau)) = 0$ and this concludes the proof of Lemma 1. ■

It follows immediately from Lemma 1 that $\mathrm{tr}\overline{\boldsymbol{Q}}(\Omega,\tau) = 0$ since the identity matrix $\boldsymbol{I}$ is of the form (53) with $b_0 = 1$ and $b_i = 0$ for $i = 1,\ldots r-1$.

Lemma 2 *Let $\boldsymbol{B} = \boldsymbol{B}(\Omega)$ be a matrix defined as in Lemma 1 and let $\boldsymbol{Q}(\Omega)$ be the $r \times r$ matrix with element (k,ℓ) defined in (51). Then, the matrix $\boldsymbol{C}(\Omega) = \boldsymbol{Q}(\Omega)\boldsymbol{B}(\Omega)$ is of the form (53).*

Proof: The element (k,ℓ) of the matrix $\boldsymbol{C} = \boldsymbol{C}(\Omega)$, $(\boldsymbol{C})_{\ell,k}$ is given by

$$\begin{aligned}(\boldsymbol{C})_{\ell,k} &= \sum_{t=1}^{r}(\boldsymbol{B})_{\ell,t}(\boldsymbol{Q}(\Omega))_{t,k}\\ &= \mathrm{e}^{j\frac{k-\ell}{r}\Omega}\kappa(\ell,k)\end{aligned} \tag{56}$$

with

$$\kappa(\ell,k) = \frac{1}{T_c^2}\sum_{s=-\mathrm{sign}(\Omega)\left\lfloor\frac{r-1}{2}\right\rfloor}^{\mathrm{sign}(\Omega)\left\lfloor\frac{r}{2}\right\rfloor}\left|\Phi\left(\frac{\Omega+2\pi s}{T_c}\right)\right|^2\eta(\ell,k,s)$$

and

$$\eta(\ell,k,s) = \sum_{t=1}^{r} b_{(r+t-\ell)\mathrm{mod}r}\mathrm{e}^{-j2\pi\left(\frac{t-k}{r}\right)s}. \tag{57}$$

In order to prove Lemma 2 it is sufficient to prove that

$$\kappa(\ell,k) = \kappa((\ell+1)\mathrm{mod}r,(k+1)\mathrm{mod}r). \tag{58}$$

In fact, in this case $\boldsymbol{C}_{\ell,k} = \mathrm{e}^{j\frac{k-\ell}{r}\Omega}\kappa_{(r+k-\ell)\mathrm{mod}r}$ with $\kappa_{(r+k-\ell)\mathrm{mod}r} = \kappa(\ell,k)$. The property (58) is implied by a similar property on $\eta(\ell,k,s)$

$$\eta(\ell,k,s) = \eta((\ell+1)\mathrm{mod}r,(k+1)\mathrm{mod}r,s). \tag{59}$$

It is straightforward to verify that (59) is satisfied since both factors $b_{(r+t-\ell)\mathrm{mod}r}$ and $\mathrm{e}^{-j2\pi\left(\frac{t-k}{r}\right)}$ are periodical in their arguments ℓ and k, respectively, with period r and k and ℓ are simultaneously increased by a unit. This concludes the proof of Lemma 2. ■

The following lemma provides the eigenvalue decomposition of the matrix $\boldsymbol{Q}(\Omega)$.

Lemma 3 *Let $\boldsymbol{Q}(\Omega)$ be an $r \times r$ matrix with element (k,ℓ) defined in (51). Then, the matrix $\boldsymbol{Q}(\Omega)$ can be decomposed as follows*

$$\boldsymbol{Q}(\Omega) = \boldsymbol{U}(\Omega)\boldsymbol{D}(\Omega)\boldsymbol{U}^H(\Omega) \tag{60}$$

where

$$\boldsymbol{U}(\Omega) = \left(\boldsymbol{e}\left(\Omega - \text{sign}(\Omega)2\pi\left\lfloor\frac{r-1}{2}\right\rfloor\right), \ldots \boldsymbol{e}\left(\Omega\right) \ldots \boldsymbol{e}\left(\Omega + \text{sign}(\Omega)2\pi\left\lfloor\frac{r}{2}\right\rfloor\right)\right), \tag{61}$$

$\boldsymbol{e}\left(\Omega\right)$ is an r-dimensional column vector defined by

$$\boldsymbol{e}\left(\Omega\right) = \frac{1}{\sqrt{r}}\left(1, \mathrm{e}^{-j\frac{\Omega}{r}}, \ldots \mathrm{e}^{-j\frac{r-1}{r}\Omega}\right)^T,$$

and $\boldsymbol{D}(\Omega)$ is the diagonal matrix whose s^{th} diagonal element is given by

$$(\boldsymbol{D}(\Omega))_{ss} = \frac{r}{T_c^2}\left|\Phi\left(\frac{1}{T_c}\left(\Omega - \text{sign}(\Omega)2\pi\left(\left\lfloor\frac{r-1}{2}\right\rfloor - s + 1\right)\right)\right)\right|^2. \tag{62}$$

Proof: Decomposition (60) can be immediately derived by noting that

$$\boldsymbol{Q}(\Omega) = \sum_{s=-\text{sign}(\Omega)\left\lfloor\frac{r-1}{2}\right\rfloor}^{\text{sign}(\Omega)\left\lfloor\frac{r}{2}\right\rfloor} \frac{r}{T_c^2}\left|\Phi\left(\frac{1}{T_c}\Omega + 2\pi s\right)\right|^2 \boldsymbol{e}(\Omega + 2\pi s)\boldsymbol{e}^H(\Omega + 2\pi s).$$

This expression can be rewritten as (60) and Lemma 3 is proven. ■

The following lemma shows that the matrix $\boldsymbol{Q}(\Omega)$ and any other matrix with the same basis of eigenvectors is of the form (53).

Lemma 4 *Let $\boldsymbol{C}(\Omega) = \boldsymbol{U}(\Omega)\boldsymbol{M}(\Omega)\boldsymbol{U}^H(\Omega)$ with $\boldsymbol{U}(\Omega)$ unitary matrix defined in (61) and $\boldsymbol{M}(\Omega)$ diagonal matrix with elements $m_{kk}(\Omega)$. Then, $\boldsymbol{C}(\Omega)$ is of the form (53).*

Proof: The ℓ^{th} row of the matrix $\boldsymbol{U}(\Omega)$ is given by

$$\boldsymbol{u}_\ell(\Omega) = \frac{1}{\sqrt{r}}\left(\mathrm{e}^{-j\frac{\ell-1}{r}\left(\Omega - \text{sign}(\Omega)2\pi\lfloor\frac{r-1}{2}\rfloor\right)}, \ldots \mathrm{e}^{-j\frac{\ell-1}{r}\left(\Omega + \text{sign}(\Omega)2\pi\lfloor\frac{r}{2}\rfloor\right)}\right)$$

and $c_{\ell k}(\Omega)$, the element (ℓ, k) of the matrix $\boldsymbol{C}$ satisfies

$$\begin{aligned} c_{\ell k}(\Omega) &= \frac{1}{r}\sum_{i=1}^{r} m_{ii}\mathrm{e}^{-j\frac{\ell-k}{r}\left(\Omega - \text{sign}(\Omega)2\pi\lfloor\frac{r-1}{2}\rfloor + 2\pi(i-1)\right)} \\ &= \widetilde{b}_{\ell k}\mathrm{e}^{-j\frac{(\ell-k)}{r}\Omega} \end{aligned} \tag{63}$$

with $\widetilde{b}_{\ell k} = \sum_{i=1}^{r} \frac{m_{ii}}{r} \mathrm{e}^{j2\pi \frac{\ell-k}{r}\left(\mathrm{sign}(\Omega)\lfloor \frac{r-1}{2} \rfloor - i + 1\right)}$. It is straightforward to verify that $\widetilde{b}_{\ell k} = \widetilde{b}_{(\ell+1) \mathrm{mod} r, (k+1) \mathrm{mod} r}$. This concludes the proof of Lemma 4. ■

The following lemmas state results from random matrix theory developed along the lines of the REFORM method proposed by Girko in [41] and [42].

Lemma 5 *[41], [43] Let $\boldsymbol{\Xi} = (\xi_{ij})_{i=1,\ldots Nq_1}^{j=1,\ldots Kq_2}$ be an $Nq_1 \times Kq_2$ matrix of complex random elements ξ_{ij} structured in NK blocks of size $q_1 \times q_2$, $\boldsymbol{\Xi}_{ij}$, i.e.*

$$\boldsymbol{\Xi} = (\boldsymbol{\Xi}_{ij})_{i=1,\ldots N}^{j=1,\ldots K}$$

and $K = \beta N$ with $\beta > 0$. Let $\widetilde{\boldsymbol{P}} = (\boldsymbol{P}_{ij})_{ij=1,\ldots p_1} = [\boldsymbol{\Xi}\boldsymbol{\Xi}^H + \alpha \boldsymbol{I}]^{-1}$ and $\widetilde{\boldsymbol{G}} = (\boldsymbol{G}_{ij})_{ij=1,\ldots p_2} = [\boldsymbol{\Xi}^H\boldsymbol{\Xi} + \alpha \boldsymbol{I}]^{-1}$, where $\boldsymbol{P}_{ij}$ and $\boldsymbol{G}_{ij}$ are complex blocks of size $q_1 \times q_1$ and $q_2 \times q_2$, respectively.

Additionally, assume

H-1 *$\boldsymbol{\Xi}_{ks}$, $k = 1, \ldots, N$, $s = 1, \ldots, K$, the random blocks of the matrix $\boldsymbol{\Xi}$ are independent.*

H-2 *All the elements of the matrix $\boldsymbol{\Xi}$ are zero mean, i.e.* $\mathrm{E}\{\boldsymbol{\Xi}\} = \boldsymbol{0}$.

H-3 $\sup_{K,N} \max_{i=1,\ldots,N} \sum_{j=1}^{K} \mathrm{E}\|\boldsymbol{\Xi}_{ij}\|^2 + \sup_{K,N} \max_{j=1,\ldots,K} \sum_{i=1}^{N} \mathrm{E}\|\boldsymbol{\Xi}_{ij}\|^2 < +\infty$,

H-4 *Lindeberg condition:* $\forall \tau > 0$

$$\lim_{K=\beta N \to \infty} \left(\max_{i=1,\ldots,N} \sum_{j=1}^{K} \mathrm{E}\left(\|\boldsymbol{\Xi}_{ij}\|^2 \chi\{\|\boldsymbol{\Xi}_{ij}\| > \tau\} \right) + \max_{j=1,\ldots,K} \sum_{i=1}^{N} \mathrm{E}\left(\|\boldsymbol{\Xi}_{ij}\|^2 \chi\{\|\boldsymbol{\Xi}_{ij}\| > \tau\} \right) \right) = 0. \tag{64}$$

Then, for $\alpha \in \mathbb{C} \backslash \mathbb{R}^-$

$$\lim_{K=\beta N \to \infty} \mathrm{E}|\boldsymbol{P}_{p\ell}(\alpha) - \boldsymbol{T}_{p\ell}(\alpha)| = 0 \qquad p, \ell = 1, \ldots, p_1$$

and

$$\lim_{K=\beta N \to \infty} \mathrm{E}|\boldsymbol{G}_{p\ell}(\alpha) - \alpha^{-1}\boldsymbol{R}_{p\ell}(\alpha)| = 0 \qquad p, \ell = 1, \ldots, p_2$$

i.e. the blocks of the matrices $\widetilde{\boldsymbol{Q}}$ and $\widetilde{\boldsymbol{G}}$ converge in the first mean to the corresponding blocks of the matrices

$$\widetilde{\boldsymbol{T}} = \mathrm{diag}((\boldsymbol{C}_{nn}^{(1)}(\alpha))^{-1})_{n=1,\ldots,N}$$

and

$$\widetilde{\boldsymbol{R}} = \mathrm{diag}((\boldsymbol{C}_{kk}^{(2)}(\alpha))^{-1})_{k=1,\ldots,K}$$

respectively. The matrix blocks $\boldsymbol{C}_{nn}^{(1)}(\alpha)$ *of size* $q_1 \times q_1$ *and* $\boldsymbol{C}_{kk}^{(2)}(\alpha)$ *of size* $q_2 \times q_2$ *are equal to*

$$\boldsymbol{C}_{nn}^{(1)}(\alpha) = \alpha \boldsymbol{I} + \sum_{j=1}^{K} \mathrm{E}\left(\boldsymbol{\Xi}_{nj}(\boldsymbol{X})_{jj}\boldsymbol{\Xi}_{nj}^{H}\right)_{\boldsymbol{X}=\alpha\widetilde{\boldsymbol{G}}} \qquad n = 1, \ldots, N \tag{65}$$

$$\boldsymbol{C}_{kk}^{(2)}(\alpha) = \boldsymbol{I} + \sum_{j=1}^{p_1} \mathrm{E}\left(\boldsymbol{\Xi}_{jk}^{H}(\boldsymbol{Y})_{jj}\boldsymbol{\Xi}_{jk}^{H}\right)_{\boldsymbol{Y}=\widetilde{\boldsymbol{P}}} \qquad k = 1, \ldots, K, \tag{66}$$

respectively.

Lemma 6 *[41], [43] Let us assume that the definitions of Lemma 5 hold and the conditions of Lemma 5 are satisfied.*

Then, the $q_1 \times q_1$ *matrices* $\boldsymbol{C}_{nn}^{(1)}(\alpha)$, $n = 1, \ldots, N$ *and the* $q_2 \times q_2$ *matrices* $\boldsymbol{C}_{kk}^{(2)}(\alpha)$, $k = 1, \ldots, K$, *defined in (65) and (66), respectively, converge as* $K = \beta N \to \infty$ *to the limit matrices*

$$\lim_{K=\beta N\to+\infty} \boldsymbol{C}_{nn}^{(1)} = \boldsymbol{\Psi}_{nn}^{(1)} \qquad n = 1, \ldots, N$$

$$\lim_{K=\beta N\to+\infty} \boldsymbol{C}_{kk}^{(2)} = \boldsymbol{\Psi}_{kk}^{(2)} \qquad k = 1, \ldots, K$$

where $\boldsymbol{\Psi}_{nn}^{(1)}$, $k = 1, \ldots, N$ *and* $\boldsymbol{\Psi}_{kk}^{(2)}$, $k = 1, \ldots, K$ *satisfy the canonical system of equations*

$$\boldsymbol{\Psi}_{nn}^{(1)} = \alpha \boldsymbol{I} + \sum_{j=1}^{K} \mathrm{E}\left\{ \boldsymbol{\Xi}_{nj} \left[\boldsymbol{\Psi}_{jj}^{(2)}\right]^{-1} \boldsymbol{\Xi}_{nj}^{H} \right\}, \qquad n = 1, \ldots, N, \tag{67}$$

$$\boldsymbol{\Psi}_{kk}^{(2)} = \boldsymbol{I} + \sum_{j=1}^{N} \mathrm{E}\left\{ \boldsymbol{\Xi}_{jk}^{H} \left[\boldsymbol{\Psi}_{jj}^{(1)}\right]^{-1} \boldsymbol{\Xi}_{jk} \right\}, \qquad k = 1, \ldots, K. \tag{68}$$

The following Lemma states the existence and uniqueness of the solution of the system of canonical equations in the class of definite positive Hermitian matrices.

Lemma 7 *[41] Let us adopt the definitions of Lemma 5 and let us assume that the conditions of Lemma 5 are satisfied. Let us consider the system of canonical equations (67) and (68). Then, the solution of the canonical system of equations (67) and (68) exists and it is unique in the class of nonnegative definite analytic matrices for* $\mathrm{Re}(\alpha) > 0$.

The following lemma due to Girko provides convergence of the eigenvalue distribution of the matrix $\boldsymbol{\Xi}\boldsymbol{\Xi}^H$ with $\boldsymbol{\Xi}$ defined in Lemma 5 to a deterministic distribution function and the corresponding Stieltjes transform.

Lemma 8 *[41] Let us adopt the definitions in Lemma 5 and let the assumptions of Lemma 5 hold. Furthermore, let $\mu_{q_1N}(x, \boldsymbol{\Xi}\boldsymbol{\Xi}^H)$ denote the normalized spectral function of the square $q_1N \times q_1N$ matrix argument, i.e. the empirical eigenvalue distribution of the matrix $\boldsymbol{\Xi}\boldsymbol{\Xi}^H$. Then, for almost all x with probability one,*

$$\lim_{N\to\infty} |\mu_{q_1N}(x, \boldsymbol{\Xi}\boldsymbol{\Xi}^H) - F_{q_1N}(x)| = 0$$

where $F_{q_1N}(x)$ is the distribution function whose Stieltjes transform is equal to

$$\int_0^{+\infty} (x+\alpha)^{-1} \mathrm{d}F_{q_1N}(x) = (q_1N)^{-1}\mathrm{tr}[\widetilde{\boldsymbol{\Psi}}]^{-1} \tag{69}$$

with $\widetilde{\boldsymbol{\Psi}} = \mathrm{diag}(\boldsymbol{\Psi}_{nn})_{n=1\ldots N}$ nonnegative definite analytic matrix for $\mathrm{Re}(\alpha) > 0$ and $\boldsymbol{\Psi}_{nn}$ satisfying the canonical system of equations (67) and (68).

Lemma 9 *[44] Let $\boldsymbol{x} = (x_1, x_2, \ldots, x_N)$ be an N-dimensional column vector of complex i.i.d. elements with zero mean and unit variance and $\boldsymbol{C}$ be an $N \times N$ complex matrix. Then, for any $p \geq 2$*

$$\mathrm{E}|\boldsymbol{x}^H\boldsymbol{C}\boldsymbol{x} - \mathrm{tr}\boldsymbol{C}|^p \leq K_p \left(\left(\mathrm{E}|x_1|^4 \mathrm{tr}\boldsymbol{C}\boldsymbol{C}^H \right)^{\frac{p}{2}} + \left(\mathrm{E}|x_1|^{2p} \mathrm{tr}(\boldsymbol{C}\boldsymbol{C}^H)^{\frac{p}{2}} \right) \right) \tag{70}$$

with K_p positive constant independent of N.

APPENDIX II
PROOF OF THEOREM 1

Let us consider the r-block-wise circulant matrices of order N, $\boldsymbol{\Phi}_k$, $k = 1, \ldots K$ defined in Theorem 1, and let us denote with $\boldsymbol{F}_N^H$ the unitary Fourier transform matrix of dimensions $N \times N$ with (ℓ, m) element given by

$$(\boldsymbol{F}_N)_{\ell,m} = \frac{1}{\sqrt{N}} \mathrm{e}^{\frac{j2\pi}{N}(\ell-1)(m-1)}. \tag{71}$$

We can extend the well known results on the diagonalization of circulant matrices[4] [31] to decompose the r-block-wise circulant matrices $\boldsymbol{\Phi}_k$, $k = 1, \ldots K$ as

$$\boldsymbol{\Phi}_k = (\boldsymbol{F}_N \otimes \boldsymbol{I}_r) \boldsymbol{\Delta}_{\phi,r}(\tau_k) \boldsymbol{F}_N \tag{72}$$

[4]A circulant matrix $\boldsymbol{C} = \mathfrak{F}(f(x))$ of order N can be decomposed as $\boldsymbol{C} = \boldsymbol{F}_N \boldsymbol{D} \boldsymbol{F}_N^H$, with $\boldsymbol{D} = \mathrm{diag}(f(0), f(\frac{2\pi}{N}), \ldots, f(2\pi\frac{(N-1)}{N}))$.

where $\boldsymbol{\Delta}_{\phi,r}(\tau_k)$ is an $rN \times N$ block diagonal matrix with ℓ^{th} block given by

$$(\boldsymbol{\Delta}_{\phi,r}(\tau_k))_{\ell,\ell} = \boldsymbol{\Delta}_{\phi,r}\left(2\pi\frac{\ell-1}{N}, \tau_k\right) \tag{73}$$

and $(\boldsymbol{F}_N \otimes \boldsymbol{I}_r)$ is a unitary matrix.

The matrix $\boldsymbol{S}$ can then be rewritten as

$$\boldsymbol{S} = (\boldsymbol{F}_N \otimes \boldsymbol{I}_r)(\boldsymbol{\Delta}_{\phi,r}(\tau_1)\widetilde{\boldsymbol{s}}_1, \boldsymbol{\Delta}_{\phi,r}(\tau_2)\widetilde{\boldsymbol{s}}_2, \ldots, \boldsymbol{\Delta}_{\phi,r}(\tau_K)\widetilde{\boldsymbol{s}}_K),$$

with $\widetilde{\boldsymbol{s}}_k = \boldsymbol{F}_N^H \boldsymbol{s}_k$. Assuming the elements of the spreading sequence $\boldsymbol{s}_k$ i.i.d. Gaussian distributed, $\widetilde{\boldsymbol{s}}_k$ is also a vector with i.i.d. Gaussian distributed elements having the same distribution as the elements of $\boldsymbol{s}_k$. Since the eigenvalues of any matrix $\boldsymbol{X}$ are invariant with respect to left multiplication by a unitary matrix $\boldsymbol{U}$ and right multiplication by $\boldsymbol{U}^H$, i.e. the eigenvalues of the matrix $\boldsymbol{X}$ coincides with the eigenvalues of the matrix $\boldsymbol{U}\boldsymbol{X}\boldsymbol{U}^H$, then the singular values of the matrices $\boldsymbol{S}$ and $\widetilde{\boldsymbol{S}} = (\boldsymbol{\Delta}_{\phi,r}(\tau_1)\widetilde{\boldsymbol{s}}_1, \boldsymbol{\Delta}_{\phi,r}(\tau_2)\widetilde{\boldsymbol{s}}_2, \ldots, \boldsymbol{\Delta}_{\phi,r}(\tau_K)\widetilde{\boldsymbol{s}}_K)$ coincide. The same properties holds for the matrices $\boldsymbol{H}$ and $\widetilde{\boldsymbol{H}} = \widetilde{\boldsymbol{S}}\boldsymbol{A}$. It is straightforward to verify that also SINR_k is invariant with respect to such a transform. In fact,

$$\begin{aligned}\mathrm{SINR}_k &= \boldsymbol{h}_k^H \left(\boldsymbol{H}_k \boldsymbol{H}_k^H + \sigma^2 \boldsymbol{I}\right)^{-1} \boldsymbol{h}_k \\ &= |a_k|^2 \widetilde{\boldsymbol{s}}_k^H \left(\widetilde{\boldsymbol{H}}_k \widetilde{\boldsymbol{H}}_k^H + \sigma^2 \boldsymbol{I}\right)^{-1} \widetilde{\boldsymbol{s}}_k\end{aligned}$$

with $\boldsymbol{H}_k$ and $\widetilde{\boldsymbol{H}}_k$ obtained from the matrices $\boldsymbol{H}$ and $\widetilde{\boldsymbol{H}}$, respectively, by suppressing the k^{th} column. Therefore, in the following we focus on the analysis of the system with transfer matrix $\widetilde{\boldsymbol{H}}$.

The matrix $\widetilde{\boldsymbol{H}}$ is a matrix structured in blocks of dimensions $r \times 1$. The block (n,k) $\widetilde{\boldsymbol{h}}_{n,k}$, $n = 1, \ldots N$ and $k = 1, \ldots K$, is given by

$$\widetilde{\boldsymbol{h}}_{n,k} = |a_k|^2 (\boldsymbol{\Delta}_{\phi,r}(\tau_k))_{nn} \widetilde{s}_{n,k}$$

where $\widetilde{s}_{n,k}$ is a Gaussian random variable with zero mean and variance $\mathrm{E}\{|\widetilde{s}_{n,k}|^2\} = \frac{1}{N}$. Additionally, the variables $\widetilde{s}_{n,k}$ are i.i.d.. Therefore, conditions H-1 and H-2 for the applicability of Lemma 5 and Lemma 6 are satisfied. Condition H-3 of Lemma 5 is satisfied. In fact,

$$\begin{aligned}\zeta &= \sup_N \left[\max_{n=1,\ldots N} \sum_{k=1}^{K} \mathrm{E}\{\|\widetilde{\boldsymbol{h}}_{nk}\|^2\} + \max_{k=1,\ldots K} \sum_{n=1}^{N} \mathrm{E}\{\|\widetilde{\boldsymbol{h}}_{nk}\|^2\}\right] \\ &\leq \sup_N \left[\max_{n=1\ldots N} \sum_{k=1}^{K} \frac{|a_k|^2}{N} \|(\boldsymbol{\Delta}_{\phi,r}(\tilde{\tau}_k))_{nn}\|^2 + \max_{k=1\ldots K} \frac{|a_k|^2}{N} \sum_{n=1}^{N} \|(\boldsymbol{\Delta}_{\phi,r}(\tau_k))_{nn}\|^2\right].\end{aligned}$$

Since the function $\Phi(\omega)$ is bounded in absolute value with finite support also $|\Phi(\Omega, \tau)|$ is upper bounded for any Ω and τ. Then, there exists a constant $C_{\mathrm{MAX}} > 0$ that satisfies $\|(\boldsymbol{\Delta}_{\phi,r}(\tau_k))_{nn}\|^2 < C_{\mathrm{MAX}}$ for any k and

n. Additionally, the elements $|a_k|$ are uniformly bounded for any k, i.e. $\exists a_{\rm MAX} > 0$ such that $|a_k|^2 \leq a_{\rm MAX}^2$ for all k. Then,

$$\zeta \leq \sup_{K=\beta N} a_{\rm MAX}^2 C_{\rm MAX} \left(\frac{K}{N}+1\right) < +\infty. \tag{74}$$

In order to verify the Lindeberg condition H-4 we focus on the limit

$$\eta = \lim_{K=\beta N\to\infty} \max_N \sum_{k=1}^{K} \mathrm{E}\left(\|\widetilde{\boldsymbol{h}}_{nk}\|^2 \chi\left(\|\widetilde{\boldsymbol{h}}_{nk}\| > \delta\right)\right)$$

for any $\delta > 0$. Let us observe that $\forall n, k$

$$\begin{aligned}\mathrm{E}\left(\|\widetilde{\boldsymbol{h}}_{nk}\|^2 \chi(\|\widetilde{\boldsymbol{h}}_{nk}\| > \delta)\right) &= |a_k|^2 \|(\boldsymbol{\Delta}_{\phi,r}(\tau_k))_{nn}\|^2 \int_{\left\{|\widetilde{s}_{nk}|^2 > \frac{\delta^2}{|a_k|^2\|\boldsymbol{\Delta}_{\phi,r}(\tau_k)\|^2}\right\}} |\widetilde{s}_{nk}|^2 \mathrm{d}F(\widetilde{s}_{nk}) \\ &\leq \frac{|a_k|^4 \|(\boldsymbol{\Delta}_{\phi,r}(\tau_k))_{nn}\|^4}{\delta^2} \int_{\{|\widetilde{s}_{nk}|\geq 0\}} |\widetilde{s}_{nk}|^4 \mathrm{d}F(\widetilde{s}_{nk})\end{aligned}$$

where $F(\widetilde{s}_{nk})$ is the cumulative distribution function of $\widetilde{s}_{nk}$. By using the fact that $\widetilde{s}_{nk}$ is a complex Gaussian variable with variance $\mathrm{E}\{|s_{nk}|^2\} = \frac{1}{N}$ and forth moment $\mathrm{E}\{|s_{nk}|^4\} = \frac{2}{N^2}$ and the bounds on $|a_k|^2$ and $\|(\boldsymbol{\Delta}_{\phi,r}(\tau_k))_{nn}\|$ it holds

$$\max_{n=1,\ldots N} \mathrm{E}\left(\|\widetilde{\boldsymbol{h}}_{nk}\|^2 \chi(\|\widetilde{\boldsymbol{h}}_{nk}\| > \delta)\right) \leq \frac{2a_{\rm MAX}^4 C_{\rm MAX}^4}{\delta^2 N^2}. \tag{75}$$

Then, $\eta = 0$ since

$$0 \leq \eta \leq \frac{2a_{\rm MAX}^4 C_{\rm MAX}^4}{\delta^2} \lim_{K=\beta N\to\infty} \sum_{k=1}^{K} \frac{1}{N^2} = 0.$$

Similarly, it can be shown that

$$\lim_{K=\beta N\to\infty} \max_{k=1,\ldots,K} \sum_{n=1}^{N} \mathrm{E}\left(\|\widetilde{\boldsymbol{h}}_{nk}\|^2 \chi(\|\widetilde{\boldsymbol{h}}_{nk}\|^2 > \delta)\right) = 0$$

and the Lindeberg condition H-4 is satisfied.

From Lemma 5, $\boldsymbol{U}_{p\ell}(\alpha), p, \ell = 1, \ldots, N$, the blocks of the matrix $\boldsymbol{U}(\alpha) = (\widetilde{\boldsymbol{H}}_k \widetilde{\boldsymbol{H}}_k^H + \alpha \boldsymbol{I})^{-1}$ converge in the first mean to $r \times r$ matrices $\boldsymbol{V}_{p\ell} = (\boldsymbol{C}_{\ell\ell}^{(1)})^{-1}\delta_{p\ell}$, $p, \ell = 1, \ldots N$, and $\boldsymbol{C}_{\ell\ell}^{(1)}$ defined similarly as in Lemma 5. Additionally, from Lemma 6 the matrices $\boldsymbol{C}_{\ell\ell}^{(1)}$ can be obtained as solution of the canonical system of equations (67) and (68) asymptotically as $K = \beta N \to \infty$. Equations (67) can be rewritten as

$$\begin{aligned}\boldsymbol{\Upsilon}_{nn}^{(1)} &= \alpha \boldsymbol{I}_r + \sum_{k=1}^{K} \mathrm{E}\left\{\widetilde{\boldsymbol{h}}_{nk} [\boldsymbol{\Upsilon}_{kk}^{(2)}]^{-1} \widetilde{\boldsymbol{h}}_{nk}^H\right\} \\ &= \alpha \boldsymbol{I}_r + \frac{1}{N} \sum_{k=1}^{K} [\boldsymbol{\Upsilon}_{kk}^{(2)}]^{-1} |a_k|^2 \boldsymbol{\Delta}_{\phi,r}\left(2\pi\frac{n-1}{N}, \tau_k\right) \boldsymbol{\Delta}_{\phi,r}^H\left(2\pi\frac{n-1}{N}, \tau_k\right) \qquad n = 1, \ldots N\end{aligned} \tag{76}$$

with $\boldsymbol{\Delta}_{\phi,r}(x,\tau)$ defined in (22) and taking into account that $(\boldsymbol{\Delta}_{\phi,r}(\tau_k))_{nn} = \boldsymbol{\Delta}_{\phi,r}\left(2\pi\frac{n-1}{N},\tau_k\right)$ in (76). Equations (68) specialize to

$$\begin{aligned}\boldsymbol{\Upsilon}_{kk}^{(2)} &= 1+\sum_{n=1}^{N}\mathrm{E}\left\{\widetilde{\boldsymbol{h}}_{nk}^{H}[\boldsymbol{\Upsilon}_{nn}^{(1)}]^{-1}\widetilde{\boldsymbol{h}}_{nk}\right\}\\ &= 1+\frac{|a_k|^2}{N}\sum_{n=1}^{N}\boldsymbol{\Delta}_{\phi,r}^{H}\left(2\pi\frac{n-1}{N},\tau_k\right)[\boldsymbol{\Upsilon}_{nn}^{(1)}]^{-1}\boldsymbol{\Delta}_{\phi,r}\left(2\pi\frac{n-1}{N},\tau_k\right)\qquad k=1,\dots K.\end{aligned}\tag{77}$$

By substituting (77) in (76) and considering the canonical system of equations as $K=\beta N\to\infty$ we obtain

$$\boldsymbol{\Upsilon}^{(1)}(\Omega)=\alpha\boldsymbol{I}_r+\beta\int_{\mathcal{S}}\frac{\lambda\boldsymbol{\Delta}_{\phi,r}(\Omega,\tau)\,\boldsymbol{\Delta}_{\phi,r}^{H}(\Omega,\tau)\,f_{|\boldsymbol{A}|^2,T}(\lambda,\tau)\mathrm{d}\,\lambda\mathrm{d}\,\tau}{1+\frac{\lambda}{2\pi}\int_{\mathcal{X}}\boldsymbol{\Delta}_{\phi,r}^{H}(\Omega,\tau)\,[\boldsymbol{\Upsilon}^{(1)}(\Omega)]^{-1}\boldsymbol{\Delta}_{\phi,r}(\Omega,\tau)\,\mathrm{d}\,\Omega}$$

with $\Omega\in[0,2\pi]$, or since $\boldsymbol{\Delta}_{\phi,r}(\Omega,\tau)$ is periodical in Ω with period 2π, Ω can equivalently varies in the interval $\mathcal{X}=[-\pi,\pi]$. Here, $\mathcal{S}$ denotes the support of the distribution function $F_{|\boldsymbol{A}|^2,T}(\lambda,\tau)$. By defining $\boldsymbol{\Upsilon}(\Omega)=[\boldsymbol{\Upsilon}^{(1)}(\Omega)]^{-1}$ we obtain (21). It follows from Lemma 6

$$\lim_{K=\beta N\to+\infty}\boldsymbol{C}_{nn}^{(1)}=\boldsymbol{\Upsilon}^{-1}\left(2\pi\frac{n}{N}\right).$$

The convergence in the first mean and thus in probability of $\mathrm{SINR}_k=\widetilde{\boldsymbol{h}}_k^{H}\boldsymbol{U}(\sigma^2)\widetilde{\boldsymbol{h}}_k$ to the quantity $\varrho=\frac{|a_k|^2}{2\pi}\int\boldsymbol{\Delta}_{\phi,r}^{H}(\Omega,\tau_k)\boldsymbol{\Upsilon}(\Omega)\boldsymbol{\Delta}_{\phi,r}(\Omega,\tau_k)\mathrm{d}\Omega$ is proven if $\eta_1=\mathrm{E}\left|\widetilde{\boldsymbol{h}}_k^{H}\boldsymbol{U}(\sigma^2)\widetilde{\boldsymbol{h}}_k-\varrho\right|$ vanishes asymptotically, i.e.

$$\lim_{\substack{K,N\to\infty\\ \frac{K}{N}\to\beta}}\eta_1=0.\tag{78}$$

The rest of the proof is focused on showing (78). Let us observe

$$\eta_1\le\mathrm{E}\left|\widetilde{\boldsymbol{h}}_k^{H}\boldsymbol{U}(\sigma^2)\widetilde{\boldsymbol{h}}_k-\widetilde{\boldsymbol{h}}_k^{H}\boldsymbol{V}\widetilde{\boldsymbol{h}}_k\right|+\mathrm{E}|\widetilde{\boldsymbol{h}}_k^{H}\boldsymbol{V}\widetilde{\boldsymbol{h}}_k-\varrho|\tag{79}$$

where the triangular inequality[5] of the spectral norm is applied and $\boldsymbol{V}=\mathrm{diag}([\boldsymbol{C}_{kk}^{(1)}(\sigma^2)]^{-1})_{k=1,\dots,N}$ is defined in Lemma 6.

By applying the submultiplicative inequality for spectral norms and the triangular inequality to the first term of (79) we obtain

[5]Given two matrices $\boldsymbol{A}$ and $\boldsymbol{B}$ with consistent dimensions the following inequalities hold:

$|\boldsymbol{AB}|\le|\boldsymbol{A}||\boldsymbol{B}|$ Submultiplicative inequality of spectral norms;

$|\boldsymbol{A}+\boldsymbol{B}|\le|\boldsymbol{A}|+|\boldsymbol{B}|$ Triangular inequality of spectral norms.

$$\begin{aligned}
\mathrm{E}|\widetilde{\boldsymbol{h}}_k^H(\boldsymbol{U}(\sigma^2)-\boldsymbol{V})\widetilde{\boldsymbol{h}}_k| &= \mathrm{E}\left|\sum_{i,\ell}\widetilde{s}_{ik}^*\boldsymbol{\Delta}_{\phi,r}^H\left(2\pi\frac{i-1}{N},\tau_k\right)(\boldsymbol{U}(\sigma^2)-\boldsymbol{V})_{i\ell}\boldsymbol{\Delta}_{\phi,r}\left(2\pi\frac{\ell-1}{N},\tau_k\right)\widetilde{s}_{\ell k}\right| \\
&\leq \sum_{i,\ell}\mathrm{E}(|(\boldsymbol{U}(\sigma^2))_{i\ell}-\boldsymbol{V}_{i\ell}|)\mathrm{E}|\widetilde{s}_{ik}^*\widetilde{s}_{\ell k}|\boldsymbol{\Delta}_{\phi,r}^H\left(2\pi\frac{i-1}{N},\tau_k\right)\boldsymbol{\Delta}_{\phi,r}\left(2\pi\frac{\ell-1}{N},\tau_k\right) \\
&= \sum_i \mathrm{E}|(\boldsymbol{U}(\sigma^2))_{ii}-\boldsymbol{V}_{ii}|\frac{\left\|\boldsymbol{\Delta}_{\phi,r}\left(2\pi\frac{i-1}{N},\tau_k\right)\right\|^2}{N} \\
&\leq \sum_i \frac{\|\boldsymbol{\Delta}_{\phi,r}\left(2\pi\frac{i-1}{N},\tau_k\right)\|^2}{N}\max_i \mathrm{E}|(\boldsymbol{U}(\sigma^2))_{ii}-\boldsymbol{V}_{ii}|.
\end{aligned}$$

Thanks to Lemma 5 and the fact that $\|\boldsymbol{\Delta}_{\phi,r}\left(2\pi\frac{i-1}{N},\tau_k\right)\|^2 \leq K_{\mathrm{MAX}}$ for all $i=1,\ldots N$ and τ_k

$$\lim_{\substack{K,N\to\infty \\ \frac{K}{N}\to\beta}} \mathrm{E}|\widetilde{\boldsymbol{h}}_k^H(\boldsymbol{U}(\sigma^2)-\boldsymbol{V})\widetilde{\boldsymbol{h}}_k| = 0.$$

In order to prove the convergence to zero of $\eta_2 = \mathrm{E}|\widetilde{\boldsymbol{h}}_k^H\boldsymbol{V}\widetilde{\boldsymbol{h}}_k - \varrho|$ we consider

$$\begin{aligned}
\eta_2^2 &\leq \mathrm{E}|\widetilde{\boldsymbol{h}}_k^H\boldsymbol{V}\widetilde{\boldsymbol{h}}_k-\varrho|^2 \\
&= \mathrm{E}((\widetilde{\boldsymbol{h}}_k^H\boldsymbol{V}\widetilde{\boldsymbol{h}}_k)^2 - 2\varrho\widetilde{\boldsymbol{h}}_k^H\boldsymbol{V}\widetilde{\boldsymbol{h}}_k+\varrho^2) \\
&= \mathrm{E}\left(|a_k|^4\sum_{ij}\boldsymbol{\Delta}_{\phi,r}^H\left(2\pi\frac{i-1}{N},\tau_k\right)\boldsymbol{V}_{ii}\boldsymbol{\Delta}_{\phi,r}\left(2\pi\frac{i-1}{N},\tau_k\right)\boldsymbol{\Delta}_{\phi,r}^H\left(2\pi\frac{j-1}{N},\tau_k\right)\boldsymbol{V}_{jj}\boldsymbol{\Delta}_{\phi,r}\left(2\pi\frac{j-1}{N},\tau_k\right)|\widetilde{s}_{ik}|^2|\widetilde{s}_{jk}|^2\right. \\
&\quad \left.-2\varrho|a_k|^2\sum_i\boldsymbol{\Delta}_{\phi,r}^H\left(2\pi\frac{i-1}{N},\tau_k\right)\boldsymbol{V}_{ii}\boldsymbol{\Delta}_{\phi,r}\left(2\pi\frac{i-1}{N},\tau_k\right)|\widetilde{s}_{ik}|^2+\varrho^2\right) \qquad (80) \\
&= \frac{2|a_k|^4}{N^2}\sum_i\left(\boldsymbol{\Delta}_{\phi,r}^H\left(2\pi\frac{i-1}{N},\tau_k\right)\boldsymbol{V}_{ii}\boldsymbol{\Delta}_{\phi,r}^H\left(2\pi\frac{i-1}{N},\tau_k\right)\right)^2+\frac{|a_k|^4}{N^2}\sum_{\substack{i,j\\ i\neq j}}\boldsymbol{\Delta}_{\phi,r}^H\left(2\pi\frac{i-1}{N},\tau_k\right)\boldsymbol{V}_{ii}\boldsymbol{\Delta}_{\phi,r}^H\left(2\pi\frac{i-1}{N},\tau_k\right) \\
&\quad \times\boldsymbol{\Delta}_{\phi,r}^H\left(2\pi\frac{j-1}{N},\tau_k\right)\boldsymbol{V}_{jj}\boldsymbol{\Delta}_{\phi,r}^H\left(2\pi\frac{j-1}{N},\tau_k\right)-\frac{2\varrho}{N}\sum_i\boldsymbol{\Delta}_{\phi,r}^H\left(2\pi\frac{i-1}{N},\tau_k\right)\boldsymbol{V}_{ii}\boldsymbol{\Delta}_{\phi,r}\left(2\pi\frac{i-1}{N},\tau_k\right)+\varrho^2. \qquad (81)
\end{aligned}$$

From (80) to (81) we make use of the assumption that $\widetilde{s}_{ij}$ is a complex Gaussian variable circularly invariant with variance N^{-1}. Let us observe that the spectral norm of $\boldsymbol{\Upsilon}(\Omega)$ and $\boldsymbol{V}_{ii}$, for any i, are bounded by $|\boldsymbol{\Upsilon}(\Omega)|<\sigma^2$ and $|\boldsymbol{V}_{ii}|<\sigma^2$. Then, the first term in (81) vanishes as $N\to\infty$. By appealing Lemma 6, for any i, $\boldsymbol{V}_{ii}\to\boldsymbol{\Upsilon}\left(2\pi\frac{i}{N}\right)$ as $K,N\to\infty$ with $\frac{K}{N}\to\beta$. Then, the second and third terms in (81) converge to ϱ^2 and $-2\varrho^2$, respectively. We can conclude that

$$\lim_{\substack{K,N\to\infty \\ \frac{K}{N}\to\beta}} \eta_2^2 = 0$$

and $\eta_2 \to 0$ as $K, N \to \infty$ as $\frac{K}{N} \to \beta$. Therefore, (78) and thus the convergence in the first mean of SINR_k is proven. The Markov inequality implies that, $\forall \varepsilon > 0$

$$\lim_{\substack{K,N\to\infty \\ \frac{K}{N}\to\beta}} \Pr\{|\widetilde{\boldsymbol{h}}_k^H \boldsymbol{U}(\sigma^2)\widetilde{\boldsymbol{h}}_k - \varrho| > \varepsilon\} \leq \frac{1}{\varepsilon} \lim_{\substack{K,N\to\infty \\ \frac{K}{N}\to\beta}} \mathrm{E}|\widetilde{\boldsymbol{h}}_k^H \boldsymbol{U}(\sigma^2)\widetilde{\boldsymbol{h}}_k - \varrho| = 0$$

and the convergence in probability stated in Theorem 1 is proven.

This concludes the proof of Theorem 1.

APPENDIX III

PROOF OF COROLLARY 2

In order to prove Corollary 2 we rewrite the limit SINR_k in (20) as

$$\lim_{K,N\to\infty} \mathrm{SINR}_k = \frac{|a_k|^2}{2\pi} \int_{-\pi}^{\pi} \mathrm{tr}\left(\boldsymbol{\Upsilon}(\Omega)\boldsymbol{Q}(\Omega,\tau_k)\right) \mathrm{d}\Omega \tag{82}$$

and the fixed point equation (21) as

$$\boldsymbol{\Upsilon}^{-1}(\Omega) = \sigma^2 \boldsymbol{I}_r + \beta \int_0^{+\infty} \int_0^{T_c} \frac{\lambda \boldsymbol{Q}(\Omega,\tau) f_{|\boldsymbol{A}|^2,T}(\lambda,\tau)\mathrm{d}\lambda\mathrm{d}\tau}{1 + \frac{\lambda}{2\pi}\int_{-\pi}^{\pi} \mathrm{tr}\left(\boldsymbol{\Upsilon}(\Omega)\boldsymbol{Q}(\Omega,\tau)\right)\mathrm{d}\Omega} \qquad -\pi \leq \Omega \leq \pi \tag{83}$$

with $\boldsymbol{Q}(\Omega,\tau)$ defined in (49). The matrix $\boldsymbol{Q}(\Omega,\tau)$ can be decomposed as in (50). Thanks to the assumptions on $\Phi(\Omega)$ in Corollary 2, the conditions on $\boldsymbol{Q}(\Omega)$ and $\overline{\boldsymbol{Q}}(\Omega,\tau)$ in Lemma 1 and Lemma 2 are satisfied. First we show that $\boldsymbol{\Upsilon}(\Omega)$, the unique solution of (83) in the class of nonnegative definite analytic functions in $\mathrm{Re}(\sigma^2) > 0$, is an $r \times r$ matrix with eigenbasis $\boldsymbol{U}(\Omega)$ defined in (61). Let us assume that $\boldsymbol{\Upsilon}(\Omega) = \boldsymbol{U}(\Omega)\widetilde{\boldsymbol{\Upsilon}}(\Omega)\boldsymbol{U}^H(\Omega)$ with elements of $\widetilde{\boldsymbol{\Upsilon}}(\Omega)$ nonnegative for all $\Omega \in [-\pi,\pi]$. By appealing to Lemma 4 $\boldsymbol{\Upsilon}(\Omega)$ is of form (53). Then, by applying Lemma 1 it results $\mathrm{tr}\left(\boldsymbol{\Upsilon}(\Omega)\overline{\boldsymbol{Q}}(\Omega,\tau)\right) = 0$ for all $\Omega \in [-\pi,\pi]$. Therefore,

$$\begin{aligned}\int_{-\pi}^{\pi} \mathrm{tr}\left(\boldsymbol{\Upsilon}(\Omega)\boldsymbol{Q}(\Omega,\tau)\right)\mathrm{d}\Omega &= \int_{-\pi}^{\pi} \mathrm{tr}\left(\boldsymbol{\Upsilon}(\Omega)\boldsymbol{Q}(\Omega)\right)\mathrm{d}\Omega \\ &= \int_{-\pi}^{\pi} \mathrm{tr}\left(\widetilde{\boldsymbol{\Upsilon}}(\Omega)\boldsymbol{D}(\Omega)\right)\mathrm{d}\Omega \geq 0\end{aligned}$$

with $\boldsymbol{D}(\Omega)$ defined as in Lemma 3. Let us notice that $\int_0^{T_c} \overline{\boldsymbol{Q}}(\Omega,\tau)\mathrm{d}F_T(\tau) = 0$ for all Ω. Thanks to this property, the assumption of independence of the random variables λ and τ and to the uniform distribution of τ (83) can be rewritten as

$$\widetilde{\boldsymbol{\Upsilon}}^{-1}(\Omega) = \sigma^2 \boldsymbol{I}_r + \beta \left(\int_0^{+\infty} \frac{\lambda \mathrm{d}F_{|\boldsymbol{A}|^2}(\lambda)}{1 + \frac{\lambda}{2\pi}\int_{-\pi}^{\pi} \mathrm{tr}\left(\widetilde{\boldsymbol{\Upsilon}}(\Omega)\boldsymbol{D}(\Omega)\right)\mathrm{d}\Omega} \right) \qquad -\pi \leq \Omega \leq \pi. \tag{84}$$

Since $\widetilde{\boldsymbol{\Upsilon}}(\Omega)$ and $\boldsymbol{D}$ are diagonal matrices, the matrix equation (83) reduces to a system of L scalar equations. Furthermore, all the quantities that appears in the right hand side of the system of equations (84) are nonnegative under the assumption that $\widetilde{\boldsymbol{\Upsilon}}(\Omega)$ is a nonnegative definite matrix and (84) admits a nonnegative definite solution for $\mathrm{Re}(\sigma^2) > 0$. The existence of a nonnegative definite solution of the system of equations (84) implies also a solution of the fixed point matrix equation (83) given by $\boldsymbol{\Upsilon}(\Omega) = \boldsymbol{U}(\Omega)\widetilde{\boldsymbol{\Upsilon}}(\Omega)\boldsymbol{U}^H(\Omega)$. Let $\widetilde{\upsilon}_s(\Omega)$ be the s^{th} diagonal element of $\widetilde{\boldsymbol{\Upsilon}}(\Omega)$ and let us recall that the s^{th} diagonal element of $\boldsymbol{D}(\Omega)$ is given in (62). Then, (84) reduces to

$$\widetilde{\upsilon}_s^{-1}(\Omega) = \sigma^2 + \beta\frac{r}{T_c^2}\left|\Phi\left(\frac{\Omega}{T_c} - \mathrm{sign}(\Omega)\frac{2\pi}{T_c}\left(\left\lfloor\frac{r-1}{2}\right\rfloor - s + 1\right)\right)\right|^2 \times \int_0^{+\infty} \frac{\lambda \mathrm{d}F_{|\boldsymbol{A}|^2}(\lambda)}{1 + \frac{\lambda r}{2\pi T_c^2}\int_{-\pi}^{\pi}\sum_{\ell=1}^{r}\widetilde{\upsilon}_\ell(\Omega)\left|\Phi\left(\frac{\Omega}{T_c} - \frac{2\pi}{T_c}\mathrm{sign}(\Omega)\left(\left\lfloor\frac{r-1}{2}\right\rfloor - \ell + 1\right)\right)\right|^2 \mathrm{d}\Omega} \quad -\pi \leq \Omega \leq \pi \text{ and } s = 1, \ldots r. \quad (85)$$

By changing the variable $y = \Omega - \mathrm{sign}(\Omega)2\pi\left(\left\lfloor\frac{r-1}{2}\right\rfloor - s + 1\right)$ and defining the function $\upsilon(y)$ in the interval $(-r\pi, r\pi)$ as follows

$$\upsilon(y) = \begin{cases} \widetilde{\upsilon}_s\left(y - 2\pi\left(\left\lfloor\frac{r-1}{2}\right\rfloor - s + 1\right)\right) & \left\lfloor\frac{r-1}{2}\right\rfloor - s + \frac{1}{2} \leq \frac{y}{2\pi} \leq \left\lfloor\frac{r-1}{2}\right\rfloor - s + 1, \\ \widetilde{\upsilon}_s\left(y + 2\pi\left(\left\lfloor\frac{r-1}{2}\right\rfloor - s + 1\right)\right) & s - 1 - \left\lfloor\frac{r-1}{2}\right\rfloor \leq \frac{y}{2\pi} \leq s - \frac{1}{2} - \left\lfloor\frac{r-1}{2}\right\rfloor \end{cases} \qquad s = 1, \ldots, r \quad (86)$$

the system of equations (85) can be rewritten as

$$\upsilon^{-1}(\Omega) = \sigma^2 + \beta\frac{r}{T_c^2}\left|\Phi\left(\frac{y}{T_c}\right)\right|^2 \int_0^{+\infty} \frac{\lambda \mathrm{d}F_{|\boldsymbol{A}|^2}(\lambda)}{1 + \frac{\lambda r}{2\pi T_c}\int_{-r\pi}^{r\pi}\upsilon(t)\left|\Phi\left(\frac{t}{T_c}\right)\right|^2 \mathrm{d}t} \qquad |y| \leq r\pi. \quad (87)$$

A similar approach applied to (82) yields

$$\begin{aligned} \lim_{K,N\to\infty} \mathrm{SINR}_k &= \frac{|a_k|^2 r}{T_c^2}\sum_{s=1}^{r}\int_{-\pi}^{\pi}\left|\Phi\left(\Omega - 2\pi\mathrm{sign}(\Omega)\left(\left\lfloor\frac{r-1}{2}\right\rfloor - s + 1\right)\right)\right|^2 \upsilon(\Omega)\mathrm{d}\Omega \\ &= \frac{|a_k|^2 r}{T_c^2}\int_{-\pi r}^{\pi r}\left|\Phi\left(\frac{\Omega}{T_c}\right)\right|^2 \upsilon(\Omega)\mathrm{d}\Omega. \end{aligned} \quad (88)$$

Let us recall that the variance of the discrete white noise is $\sigma^2 = \frac{N_0 r}{T_c}$. Additionally, let us define the function

$$\eta\left(\frac{\Omega}{T_c}\right) = \frac{r N_0}{T_c E_\phi}\left|\Phi\left(\frac{\Omega}{T_c}\right)\right|^2 \upsilon(\Omega). \quad (89)$$

By substituting (19) in (87) and (88), using definition (89), and $\omega = \frac{\Omega}{T_c}$ we obtain the fixed point equation (26) and the limit (25), respectively. This concludes the proof of Corollary 2.

APPENDIX IV
PROOF OF THEOREM 2

The proof of Theorem 2 follows along the line of the proof of Theorem 1. In this case $\boldsymbol{\Delta}_{\phi,r}(\Omega,\tau) = \frac{\mathrm{e}^{j\frac{\sqrt{r}}{T_c}\tau\Omega}}{T_c}\Phi^*\left(\frac{\Omega}{T_c}\right)\boldsymbol{e}(\Omega)$ and the matrix $\boldsymbol{Q}(\Omega,\tau)$ is independent of τ. Specifically,

$$\boldsymbol{Q}(\Omega,\tau) = \frac{r}{T_c^2}\left|\Phi\left(\frac{\Omega}{T_c}\right)\right|^2 \boldsymbol{e}(\Omega)\boldsymbol{e}^H(\Omega).$$

Then, applying the same approach as in Theorem 1 Lemma 5 and Lemma 6 yield

$$\lim_{K,N\to\infty}\mathrm{SINR}_k = \frac{|a_k|^2 r}{2\pi T_c^2}\int_{-\pi}^{\pi}\left|\Phi\left(\frac{\Omega}{T_c}\right)\right|^2 \boldsymbol{e}^H(\Omega)\widetilde{\boldsymbol{\Upsilon}}(\sigma^2,\Omega)\boldsymbol{e}(\Omega)\mathrm{d}\Omega$$

with

$$\begin{aligned}\widetilde{\boldsymbol{\Upsilon}}^{-1}(\sigma^2,\Omega) &= \sigma^2\boldsymbol{I}_r + \beta\frac{r}{T_c^2}\left|\Phi\left(\frac{\Omega}{T_c}\right)\right|^2 \boldsymbol{e}(\Omega)\boldsymbol{e}^H(\Omega)\int_0^{+\infty}\frac{\lambda\mathrm{d}F_{|A|^2}(\lambda)}{1+\frac{\lambda}{2\pi}\int_{-\pi}^{\pi}\frac{r}{T_c^2}\left|\Phi\left(\frac{\Omega}{T_c}\right)\right|^2 \boldsymbol{e}^H(\Omega)\widetilde{\boldsymbol{\Upsilon}}(\sigma^2,\Omega)\boldsymbol{e}(\Omega)\mathrm{d}\Omega} \\ &= \sigma^2\boldsymbol{I}_r + \beta\int_0^{+\infty}\frac{\boldsymbol{U}(\Omega)\boldsymbol{D}'(\Omega)\boldsymbol{U}^H(\Omega)\lambda\mathrm{d}F_{|\boldsymbol{A}|^2}(\lambda)}{1+\frac{\lambda}{2\pi}\int_{-\pi}^{\pi}\frac{r}{T_c^2}\left|\Phi\left(\frac{\Omega}{T_c}\right)\right|^2 \boldsymbol{e}^H(\Omega)\widetilde{\boldsymbol{\Upsilon}}(\sigma^2,\Omega)\boldsymbol{e}(\Omega)\mathrm{d}\Omega} \qquad (90)\end{aligned}$$

with $\boldsymbol{U}(\Omega)$ defined in (61) and $\boldsymbol{D}'(\Omega)$ diagonal matrix with all zero elements except the $\left(\left\lfloor\frac{r-1}{2}\right\rfloor+1\right)^{\mathrm{th}}$ element, corresponding to the eigenvector $\boldsymbol{e}(\Omega)$ and equal to $\frac{r}{T_c^2}\left|\Phi\left(\frac{\Omega}{T_c}\right)\right|^2$. Then, it is apparent that the solution of the fixed point matrix equation (90) is a matrix with the basis of eigenvectors $\boldsymbol{U}(\Omega)$ and (90) reduces to the equation corresponding to the $\left(\left\lfloor\frac{r-1}{2}\right\rfloor+1\right)^{\mathrm{th}}$ element $\upsilon(\Omega)$ of $\boldsymbol{\Upsilon}(\Omega) = \boldsymbol{U}^H(\Omega)\widetilde{\boldsymbol{\Upsilon}}(\Omega)\boldsymbol{U}(\Omega)$

$$\upsilon_s^{-1}(\Omega) = \sigma^2 + \beta\frac{r}{T_c^2}\left|\Phi\left(\frac{\Omega}{T_c}\right)\right|^2\int\frac{\lambda\mathrm{d}F_{|\boldsymbol{A}|^2}(\lambda)}{1+\frac{\lambda r}{2\pi T_c^2}\int_{-\pi}^{\pi}\left|\Phi\left(\frac{\Omega}{T_c}\right)\right|^2\upsilon(\Omega)\mathrm{d}\Omega}. \qquad (91)$$

The other components of the diagonal matrix $\boldsymbol{\Upsilon}(\Omega)$ are simply given by $\upsilon_s^{-1}(\Omega) = \sigma^2$, $s = 1,\ldots,r$ and $s \neq \left(\left\lfloor\frac{r-1}{2}\right\rfloor+1\right)$. The identity $\boldsymbol{e}^H(\Omega)\widetilde{\boldsymbol{\Upsilon}}(\Omega)\boldsymbol{e}(\Omega) = \upsilon(\Omega)$ yields

$$\lim_{K=\beta N\to\infty}\mathrm{SINR}_k = \frac{|a_k|^2 r}{2\pi T_c^2}\int_{-\pi}^{\pi}\left|\Phi\left(\frac{\Omega}{T_c}\right)\right|^2\upsilon(\Omega)\mathrm{d}\Omega. \qquad (92)$$

The convergence (92) in probability or in the first mean can be proven as in Theorem 1. By substituting (19) in (91) and (92), using definition (89), and $\omega = \frac{\Omega}{T_c}$, we obtain the fixed point equation (36) and the limit (35), respectively.

This concludes the proof of Theorem 2.

APPENDIX V
PROOF OF PROPOSITION 2

Proposition 2 follows immediately from Corollary 3. In fact, from (33) it is apparent that the multiuser efficiency of a system with load β and sinc pulses having roll-off equal to α is equal to the multiuser efficiency of a system with load $\frac{\beta}{\alpha}$ and sinc pulses having zero roll-off. Thanks to the fundamental relations between multiuser efficiency and capacity [39] we obtain (41). Since the spectral efficiency is obtained as the ratio $\frac{\mathcal{C}^{(\text{sinc})}(\beta, \text{SNR}, \alpha)\big|_{\text{SNR}=N_0^{-1}}}{\alpha}$, it is apparent from (41) that it is constant as $\beta \to \infty$ for any finite bandwidth α.

APPENDIX VI
PROOF OF COROLLARY 4

Let $\text{MMSE}_{b_k[m]}(\rho)$ be the achievable MMSE by an estimator of the symbol $b_k[m]$ transmitted by user k in the m-th symbol interval when the transmitted signal $\boldsymbol{b}$ in (14) is Gaussian and the signal to noise ratio is $\rho = \sigma^{-2}$. Furthermore, let $\text{SINR}_{b_k[m]}(\rho)$ be the SINR at the output of the same MMSE estimator for the transmitted symbol $b_k[m]$. Then,

$$\text{MMSE}_{b_k[m]}(\rho) = \frac{1}{1 + \text{SINR}_{b_k[m]}(\rho)}. \tag{93}$$

Additionally, let $I(\boldsymbol{b}; \boldsymbol{y}, \rho)$ be the mutual information in nats between the input $\boldsymbol{b}$ and the output $\boldsymbol{y}$. From Theorem 2 in [39] the following relation holds

$$\frac{\text{d}}{\text{d}\rho} I(\boldsymbol{b}; \boldsymbol{y}, \rho) = \text{E}\{\|\boldsymbol{H}\boldsymbol{b} - \boldsymbol{H}\widehat{\boldsymbol{b}}\|^2\} \tag{94}$$

being $\widehat{\boldsymbol{b}}$ the conditional mean estimate. We recall here that for Gaussian signals conditional mean estimate and MMSE estimate coincide (see e.g. [35]) and

$$\begin{aligned} \text{E}\{\|\boldsymbol{H}\boldsymbol{b} - \boldsymbol{H}\widehat{\boldsymbol{b}}\|^2\} &= \text{tr}\sigma^2 \boldsymbol{H}^H (\boldsymbol{H}\boldsymbol{H}^H + \sigma^2 \boldsymbol{I})^{-1} \boldsymbol{H} \\ &= \sum_{m,k} \frac{\text{SINR}_{b_k[m]}(\rho)}{\rho(1 + \text{SINR}_{b_k[m]}(\rho))}. \end{aligned} \tag{95}$$

For $K, N, m \to \infty$ with $\frac{K}{N} \to \beta$, $\text{SINR}_{b_k[m]}(\rho)$ converges with probability one to deterministic values. More specifically, $\text{SINR}_{b_k[m]}(\rho) = \frac{|a_k|^2 E_\phi}{N_0} \eta_\gamma \Big|_{\gamma = \frac{r\rho}{T_c}}$, being η_γ the multiuser efficiency corresponding to $\gamma = \frac{E_\phi}{N_0}$ as in Corollary 2 or Theorem 2.

Then, the total capacity per chip constrained to a given chip pulse waveform is given by

$$\mathcal{C}^{(\text{asyn})}\left(\beta, \frac{E_\phi}{N_0}, \phi\right) = \frac{\beta}{\ln 2}\int_0^{\frac{E_\phi T_c}{rN_0}} \int_0^{+\infty} \frac{\lambda \frac{rs}{T_c}\eta_{\frac{rs}{T_c}} \mathrm{d}F_{|\boldsymbol{A}|^2}(\lambda)\,\mathrm{d}s}{1+\lambda\frac{rs}{T_c}\eta_{\frac{rs}{T_c}}} \tag{96}$$

$$= \frac{\beta}{\ln 2}\int_0^{\frac{E_\phi}{N_0}} \mathrm{d}t \int_0^{+\infty} \frac{\lambda\eta_t \mathrm{d}F_{|\boldsymbol{A}|^2}(\lambda)}{1+\lambda t\eta_t} \tag{97}$$

This concludes the proof of Corollary 4.

APPENDIX VII

PROOF OF THEOREM 3

In this section $\mathbf{0}_N^M$ denotes an $N \times M$ matrix of zeros. Shortly, $\mathbf{0}_N$ and $\boldsymbol{e}_N$ denote N-dimensional vectors of zeros and ones, respectively. Additionally, we introduce the notation $\boldsymbol{F}_N^{(r)} = \boldsymbol{F}_N \otimes \boldsymbol{I}_r$, with $\boldsymbol{F}_N$ already defined in (71).

A basic property of the Fourier eigenbasis functions is stated in the following.

Property 1 *Let $\boldsymbol{E}_L$ denote an $L \times L$ matrix of ones and by $\boldsymbol{\mathcal{F}}_L^{(r)}(u)$, with $u \leq (L-1)Nr$, the $LNr \times LN$ matrix with structure*

$$\boldsymbol{\mathcal{F}}_L^{(r)}(u) = \begin{pmatrix} \mathbf{0}_{ur}^{ur} & \mathbf{0}_{ur}^{Nr} & \mathbf{0}_{ur}^{(L-1)N-u} \\ \mathbf{0}_{Nr}^{ur} & \boldsymbol{F}_N^{(r)} & \mathbf{0}_{Nr}^{(L-1)N-u} \\ \mathbf{0}_{ur}^{(L-1)N-u} & \mathbf{0}_{Nr}^{(L-1)N-u} & \mathbf{0}_{(L-1)N-u}^{(L-1)N-u} \end{pmatrix}$$

Then,

$$\frac{1}{\sqrt{L}}(\boldsymbol{E}_L \otimes \boldsymbol{F}_N^{(r)})\boldsymbol{\mathcal{F}}_L^{(r)}(u) = \boldsymbol{\mathcal{E}}(u, r, N) \tag{98}$$

where $\boldsymbol{\mathcal{E}}(u, r, N)$ is a matrix with structure

$$\boldsymbol{\mathcal{E}}(u, r, N) = \left(\begin{array}{c|c|c} & \boldsymbol{\mathcal{R}}_{rN}^u & \\ \mathbf{0}_{LNr}^{ur} & \vdots & \mathbf{0}_{(L-1)Nr-ur}^{(L-1)Nr-ur} \\ & \boldsymbol{\mathcal{R}}_{rN}^u & \end{array}\right)$$

and $\boldsymbol{\mathcal{R}}_{rN}^u$ is an $rN \times N$ block diagonal matrix with ℓ-th block $(\boldsymbol{\mathcal{R}}_{rN}^u)_{\ell\ell} = \mathrm{e}^{-j\frac{2\pi}{N}(\ell-1)u}\boldsymbol{e}_r$.

Let us consider the virtual spreading sequence of user k for symbol m in the time interval $[-MT_s, MT_s]$, with $M > m$ integer:

$$\boldsymbol{\mathfrak{h}}_k^{(m)T} = a_k[\mathbf{0}_{(M+m)Nr}^T, \widetilde{\boldsymbol{\Phi}}_k \boldsymbol{s}_k^{(m)}, \mathbf{0}_{(M-m-1)Nr}^T].$$

Property 1 and decomposition (72) yield

$$\frac{1}{\sqrt{2M+1}}(\boldsymbol{E}_{2M+1}\otimes\boldsymbol{F}_N^{(r)})\mathfrak{h}_k^{(m)} = \boldsymbol{e}_{2M+1}\otimes(\boldsymbol{\mathcal{R}}_{rN}^{\overline{\tau}_k}\boldsymbol{\Delta}_{\phi,r}(\widetilde{\tau}_k)\widetilde{\boldsymbol{s}}_k)$$
$$= \frac{1}{\sqrt{2M+1}}(\boldsymbol{E}_{2M+1}\otimes\boldsymbol{F}_N^{(r)})\widehat{\mathfrak{h}}_k^{(m)} \tag{99}$$

with $\widehat{\mathfrak{h}}_k^{(m)} = a_k[\boldsymbol{0}_{(M+m)Nr}^T, (\boldsymbol{F}_N^{(r)}\boldsymbol{\mathcal{R}}_{rN}^{\overline{\tau}_k}\boldsymbol{\Delta}_{\phi,r}(\widetilde{\tau}_k)\widetilde{\boldsymbol{s}}_k)^T, \boldsymbol{0}_{(M-m)Nr}^T]^T$. Let us observe that the position of the nonzero elements does not depends anymore on $\overline{\tau}$. Since the random entries of the vector $\widetilde{\boldsymbol{s}}_k$ are rotationally invariant, the rotation matrix $\boldsymbol{\mathcal{R}}_{rN}^{\overline{\tau}_k}$ can be absorbed in the random vector $\widetilde{\boldsymbol{s}}_k$ without change of the statistics and the vector $\widehat{\mathfrak{h}}_k$ can be rewritten as

$$\widehat{\mathfrak{h}}_k = a_k[\boldsymbol{0}_{(M+m)Nr}, \boldsymbol{h}_k^{(m)}, \boldsymbol{0}_{(M-m)Nr}]^T$$

where $\boldsymbol{h}_k^{(m)} = \boldsymbol{F}_N^{(r)}\boldsymbol{\Delta}_{\phi,r}(\widetilde{\tau}_k)$ is the virtual spreading for the m-th transmitted symbol of user k delayed by $\widetilde{\tau} \in [0, T_c)$. From the previous considerations it follows that the random matrix $\boldsymbol{\mathcal{T}} = \boldsymbol{\mathcal{H}}\boldsymbol{\mathcal{H}}^H$ is unitarily equivalent to an infinite block diagonal matrix with blocks $\boldsymbol{T}^{(m)} = \boldsymbol{H}^{(m)}\boldsymbol{H}^{(m)H}$ of dimension $rN \times rN$ being $\boldsymbol{H}^{(m)}$ the matrix with k-th column equal to $\boldsymbol{h}_k^{(m)}$, i.e. the transfer matrix of a symbol synchronous but chip asynchronous system with time delay $\{\widetilde{\tau}_1, \ldots, \widetilde{\tau}_K\}$. Then, asymptotically for $K, N \to +\infty$ the eigenvalue distribution of the matrix $\boldsymbol{T}^{(m)}$ equals the eigenvalue distribution of the matrix $\boldsymbol{\mathcal{T}}$. The equivalence of the systems in terms of SINR at the output of a linear MMSE detector and in terms of capacity follows also from the fact that the SINR is invariant to any unitary transform of the system transfer matrix as already observed in the proof of Theorem 1.

This concludes the proof of Theorem 3.

REFERENCES

[1] M. Rupf and J. L. Massey, "Optimum sequences multisets for synchronous code–division multiple–access channels," *IEEE Transactions on Information Theory*, vol. 40, no. 4, pp. 1261–1266, July 1994.

[2] P. Viswanath, V. Anantharam, and D. N. Tse, "Optimal sequences, power control and user capacity of synchronous CDMA systems with linear MMSE multiuser receivers," *IEEE Transactions on Information Theory*, vol. 45, no. 6, pp. 1968–1983, Sept. 1999.

[3] P. Viswanath and V. Anantharam, "Optimal sequences and sum capacity of synchronous CDMA systems," *IEEE Transactions on Information Theory*, vol. 45, no. 6, pp. 1984–1991, Sept. 1999.

[4] S. Verdú and S. Shamai (Shitz), "Spectral efficiency of CDMA with random spreading," *IEEE Transactions on Information Theory*, vol. 45, no. 2, pp. 622–640, Mar. 1999.

[5] D. Tse and S. Hanly, "Linear multiuser receivers: Effective interference, effective bandwidth and user capacity," *IEEE Transactions on Information Theory*, vol. 45, no. 2, pp. 641–657, Mar. 1999.

[6] R. R. Müller, "Multiuser receivers for randomly spread signals: Fundamental limits with and without decision–feedback," *IEEE Transactions on Information Theory*, vol. 47, no. 1, pp. 268–283, Jan. 2001.

[7] S. Shamai (Shitz) and S. Verdú, "The impact of frequency–flat fading on the spectral efficiency of CDMA," *IEEE Transactions on Information Theory*, vol. 47, no. 4, pp. 1302–1327, May 2001.

[8] T. Tanaka, "A statistical mechanics approach to large-system analysis of CDMA multiuser detectors," *IEEE Transactions on Information Theory*, vol. 48, no. 11, pp. 2888–2910, Nov. 2002.

[9] A. J. Grant and P. D. Alexander, "Random sequence multisets for synchronous code–division multiple–access channels," *IEEE Transactions on Information Theory*, vol. 44, no. 7, pp. 2832–2836, Nov. 1998.

[10] M. B. Pursley, "Performance evaluation for phase–coded spread–spectrum multiple–access communication — Part I: System analysis," *IEEE Transactions on Communications*, vol. COM–25, no. 8, pp. 795–799, Aug. 1977.

[11] G. Zang and C. Ling, "Performance evaluation for band-limited DS-CDMA systems based on simplified improved Gaussian approximation," *IEEE Transactions on Communications*, vol. 51, no. 7, pp. 1204–1213, July 2003.

[12] Y. K. Jeong, J. H. Cho, and J. S. Lehnert, "An asymptotic analysis of band-limited DS/SSMA communication systems," *IEEE Transactions on Information Theory*, vol. 52, no. 2, pp. 759–766, Feb. 2006.

[13] P. Schramm and R. R. Müller, "Spectral efficiency of CDMA systems with linear MMSE interference suppression," *IEEE Transactions on Communications*, vol. 47, no. 5, pp. 722–731, May 1999.

[14] J. Luo, S. Ulukus, and A. Ephremides, "Optimal sequences and sum capacity of symbol asynchronous CDMA systems," *IEEE Transactions on Information Theory*, vol. 51, no. 8, pp. 2760–2769, Aug. 2005.

[15] Kiran and D. N. Tse, "Effective interference and effective bandwidth of linear multiuser receivers in asynchronous CDMA systems," *IEEE Transactions on Information Theory*, vol. 46, no. 4, pp. 1426–1447, Sept. 2000.

[16] Laura Cottatellucci, Merouane Debbah, and R. R. Müller, "Asymptotic analysis of linear detectors for asynchronous CDMA systems," in *Proc. of IEEE International Symposium on Information Theory (ISIT)*, Chicago, Illinois, June/July 2004.

[17] L. Cottatellucci, R. R. Müller, and M. Debbah, "Efficient implementation of multiuser detectors for asynchronous CDMA," in *Proc. 42nd Allerton Conf. on Communication, Control and Computing*, Monticello, Illinois, Sept./Oct. 2004, pp. 357–366.

[18] A. Mantravadi and V. V. Veeravalli, "MMSE detection in asynchronous CDMA systems: An equivalence result," *IEEE Transactions on Information Theory*, vol. 48, no. 12, pp. 3128–3137, Dec. 2002.

[19] U. Madhow and M. L. Honig, "MMSE interference suppression for direct–sequence spread–spectrum CDMA," *IEEE Transactions on Communications*, vol. 42, no. 12, pp. 3178–3188, Dec. 1994.

[20] ——, "On the average near–far resistance for MMSE detection of direct sequence CDMA signals with random spreading," *IEEE Transactions on Information Theory*, vol. 45, no. 6, pp. 2039–2045, Sept. 1999.

[21] S. Verdú, "Minimum probability of error for asynchronous Gaussian multiple–access channels," *IEEE Transactions on Information Theory*, vol. IT–32, no. 1, pp. 85–96, Jan. 1986.

[22] R. Lupas and S. Verdú, "Near–far resistance of multiuser detectors in asynchronous channels," *IEEE Transactions on Communications*, vol. COM–38, no. 4, pp. 496–508, Apr. 1990.

[23] M. Rupf, F. Tarköy, and J. L. Massey, "User–separating demodulation for code–division multiple–access systems," *IEEE Journal on Selected Areas in Communications*, vol. 12, no. 5, pp. 786–795, June 1994.

[24] C. Hwang, "Eigenvalue distribution of correlation matrix in asynchronous CDMA with infinite observation window width," in *Proc. of IEEE International Symposium on Information Theory (ISIT)*, Nice, France, June 2007.

[25] A. Mantravadi and V. V. Veeravalli, "On chip-matched filtering and discrete sufficient statistics for asynchronous band-limited CDMA systems," *IEEE Transactions on Communications*, vol. 49, no. 8, pp. 1457–1467, Aug. 2001.

[26] M. A. Landolsi and W. E. Stark, "DS-CDMA chip waveform design for optimal power-bandwidth performance," in *Proc. of 6th International Symposium Personal, Indoor and Mobile Radio Communications*, Toronto, ON, Sept. 1995, pp. 706–710.

[27] ——, "DS-CDMA chip waveform design for minimal interference under bandwidth , phase and envelope constraints," *IEEE Transactions on Communications*, vol. 47, no. 11, pp. 1737–1746, Nov. 1999.

[28] S. Verdú, *Multiuser Detection*. New York: Cambridge University Press, 1998.

[29] S. Verdú, "Multiuser detection," in *Advances in Statistical Signal Processing: Signal Detection*, H. Poor and J. Thomas, Eds. Greenwich, CT: JAI Press, 1993, pp. 369–410.

[30] R. M. Gray, Ed., *Toeplitz and Circulant Matrices: A Review*. Standford, CA: http://ee.standford.edu/ $\sim$ gray/toeplitz.pdf, 2002.

[31] R. M. Gray, "Toeplitz and circulant matrices: A review," *IEEE Transactions on Information Theory*, vol. 18, no. 6, pp. 725–730, Nov. 1972.

[32] J. Evans and D. N. Tse, "Large system performance of linear multiuser receivers in multipath fading channels," *IEEE Transactions on Information Theory*, vol. 46, no. 6, pp. 2059–2078, Sept. 2000.

[33] L. Li, A. Tulino, and S. Verdú, "Design of reduced-rank MMSE multiuser detectors using random matrix methods," *IEEE Transactions on Information Theory*, vol. 50, no. 6, pp. 986 – 1008, June 2004.

[34] L. Cottatellucci and R. R. Müller, "A systematic approach to multistage detectors in multipath fading channels," *IEEE Transactions on Information Theory*, vol. 51, no. 9, pp. 3146–3158, Sept. 2005.

[35] S. Kay, *Fundamentals of Statistical Signal Processing, Estimation Theory*, ser. Prentice Hall Signal Processing Series. Prentice Hall, 1993, vol. 1.

[36] R. R. Müller and W. H. Gerstacker, "On the capacity loss due to separation of detection and decoding," *IEEE Transactions on Information Theory*, vol. 50, no. 8, pp. 1769–1778, Aug. 2004.

[37] D. Guo and S. Verdú, "Randomly spread CDMA: Asymptotics via statistical physics," *IEEE Transactions on Information Theory*, vol. 51, no. 6, pp. 1983–2010, June 2005.

[38] S. V. Hanly and D. N. Tse, "Resource pooling and effective bandwidth in CDMA networks with multiuser receivers and spatial diversity," *IEEE Transactions on Information Theory*, vol. 47, no. 4, pp. 1328–1351, May 2001.

[39] D. Guo and S. Verdú, "Mutual information and minimum mean-square error in Gaussian channels," *IEEE Transactions on Information Theory*, vol. 51, no. 4, pp. 1261–1282, Apr. 2005.

[40] S. Verdú, "Capacity region of Gaussian CDMA channels: The symbol–synchronous case," in *Proc. of 24th Annual Allerton Conference on Communication, Control and Computing*, Monticello, IL, Oct. 1986, pp. 1025–1034.

[41] V. L. Girko, *Theory of Stochastic Canonical Equations*. Dordrecht, The Netherlands: Kluwer Academic Publishers, 2001, vol. 1.

[42] ——, *Theory of Stochastic Canonical Equations*. Dordrecht, The Netherlands: Kluwer Academic Publishers, 2001, vol. 2.

[43] L. Cottatellucci and R. R. Müller, "CDMA systems with correlated spatial diversity: A generalized resource pooling result." *IEEE Transactions on Information Theory*, vol. 53, no. 3, pp. 1116–1136, Mar. 2007.

[44] Z. D. Bai and J. W. Silverstein, "No eigenvalues outside the support of the limiting spectral distribution of large dimensional sample covariance matrices," *The Annals of Probability*, vol. 26, no. 1, pp. 316–345, 1998.